FACULTY OF ENGINEERING AND ARCHITECTURE

Evaluating the Total Human Electromagnetic Exposure in a UAV-aided Network

Thomas Detemmerman
Student number: 01707806

Supervisors: Prof. dr. ir. Wout Joseph, Prof. dr. ir. Luc Martens
Counsellors: Dr. ir. Margot Deruyck, German Dario Castellanos Tache

Master's dissertation submitted in order to obtain the academic degree of
Master of Science in Information Engineering Technology

Academic year 2019-2020

GHENT UNIVERSITY

Acknowledgement

To do, thanks for...

Evaluatie van de totale electromagnetische blootstelling van de mens in een netwerk van drones

door

Thomas Detemmerman

Masterproef ingediend tot het behalen van de academische graad van Master of Science in de industriële wetenschappen: informatica

Academiejaar 2019-2020

Promotoren: Prof. dr. ir. Wout Joseph, Prof. dr. ir. Luc Martens

Begeleider: Dr. ir. Margot Deruyck, MPhil. German Dario Castellanos Tache

Faculteit Ingenieurswetenschappen en architectuur

Universiteit Gent

Samenvatting

De hedendaagse samenleving vertrouwt meer dan ooit op de aanwezigheid van draadloze netwerken. Tevens groeit ook de bezorgdheid bij de menigte over de electromagnetische straling die hierbij gebruikt wordt. De overheid hanteerd dan ook strenge richtlijnen waaraan mobiele toestellen en zendmasten moeten voldoen.

Dit onderzoek tracht de specifieke absorptie snelheid van elektromagnetische straling in kaart te brengen door rekening te houden met alle mobiele toestellen en zendmasten. Om dit te verwezelijken wordt gebruik gemaakt van een tool ontwikkeld door de onderzoeksgroep WAVES aan de UGent. Deze tool simmuleert een volledig netwerk waarbij zendmasten bevestigd worden aan drones. Dit onderzoek observeert verder hoe deze drones kunnen worden aangestuurd zodoende dat bepaalde doelstellingen zoals het minimaliseren van energieverbruik of electromagnetische straling bereikt kunnen worden.

Uit de resultaten blijkt dat...

Trefwoorden

LTE, electromagnetische blootstelling, energieverbruik, drone, femtocell, microstrip patch antenna, stralingspatronen, specific absorption rate (SAR)

Evaluating the Total Human Electromagnetic Exposure in a UAV-aided Network

by
Thomas Detemmerman

Master's dissertation submitted in order to obtain the academic degree of Master of Science in Information Engineering Technology industriële wetenschappen: informatica
Academiejaar 2019-2020

Supervisors: Prof. dr. ir. Wout Joseph, Prof. dr. ir. Luc Martens
Counsellors: Dr. ir. Margot Deruyck, MPhil. German Dario Castellanos Tache
Faculty of engineering and architecture
Ghent University

Samenvatting

Society relies more than ever on the availability of the wireless networks but is at the same time also concerned about the potential health effects of the electromagnetic radiation caused by these networks. The government has enforced strict legislations to which mobile devices and base stations have to satisfy.

This research investigates the specific absorption rate caused by these electromagnetic waves by taking all mobile devices and base stations into account. To accomplish this goal, the deployment tool developed by the WAVES research group at Ghent University will be used. This tool simulates an entire network where transmission towers are represented by femtocell base stations attached to drones. This research also investigates how these drones can be guided in order to reach certain goals like minimizing power consumption or electromagnetic exposure.

It looks from the results that ... (todo)

Trefwoorden

LTE, Electromagnetic Radiation, power consumption, drones, femtocell, microstrip patch antenna, radiation pattern, specific absorption rate (SAR)

Evaluatie van de totale electromagnetische blootstelling van de mens in een netwerk van drones

Thomas Detemmerman

Supervisor(s): Wout Joseph, Luc Martens, Luc Martens, German Dario Castellanos Tache

Abstract— De hedendaagse samenleving vertrouwt meer dan ooit op de aanwezigheid van draadloze netwerken. Tevens groeit ook de bezorgdheid bij de menigte over de electromagnetische straling die hierbij gebruikt wordt. De overheid hanteerd dan ook strenge richtlijnen waaraan mobiele toestellen en zendmasten moeten voldoen.

Dit onderzoek tracht de specifieke absorptie snelheid van elektromagnetische straling in kaart te brengen door rekening te houden met alle mobiele toestellen en zendmasten. Om dit te verwezelijken wordt gebruik gemaakt van een tool ontwikkeld door de onderzoeksgroep WAVES aan de UGent. Deze tool simmuleert een volledig netwerk waarbij zendmasten bevestigd worden aan drones. Dit onderzoek observeert verder hoe deze drones kunnen worden aangestuurd zodoende dat bepaalde doelstellingen zoals het minimaliseren van energieverbruik of electromagnetische straling bereikt kunnen worden.

Uit de resultaten blijkt dat...

Keywords— LTE, electromagnetische blootstelling, energieverbruik, drone, femtocell, microstrip patch antenna, radiation pattern, specific absorption rate (SAR)

I. Introductie

THE Introduction in Dutch

II. Section

A. Gerelateerd werk

TODO

B. Scenario's

todo

C. Electromagnetische blootstelling

todo

III. Resultaten

todo

IV. Conclusie

todo

A. Referencies

todo

References

[1] Bart Lannoo, Didier Colle, Mario Pickavet, Piet Demeester, Optical Switching Architecture to Implement Moveable Cells in a Multimedia Train Environment, Proc. of ECOC 2004, 30th European Conf. on Optical Communication, vol. 3, pp. 344-345, Stockholm, Sweden, 5-9 Sep. 2004.

[2] Michael Neufeld, Ashish Jain, Dirk Grunwald, Nsclick:: bridging network simulation and deployment, http://systems.cs.colorado.edu/Networking/nsclick/

[3] The Click Modular Router Project, http://www.read.cs.ucla.edu/click/

[4] NS – Network Simulator, http://nsnam.isi.edu/nsnam/

Evaluating the Total Human Electromagnetic Exposure in a UAV-aided Network

Thomas Detemmerman

Supervisor(s): Wout Joseph, Luc Martens, Luc Martens, German Dario Castellanos Tache

Abstract— Society relies more than ever on the availability of the wireless networks but is at the same time also concerned about the potential health effects of the electromagnetic radiation caused by these networks. The government has enforced strict legislations to which mobile devices and base stations have to satisfy.

This research investigates the specific absorption rate caused by these electromagnetic waves by taking all mobile devices and base stations into account. To accomplish this goal, the deployment tool developed by the WAVES research group at Ghent University will be used. This tool simulates an entire network where transmission towers are represented by femtocell base stations attached to drones. This research also investigates how these drones can be guided in order to reach certain goals like minimizing power consumption or electromagnetic exposure.

It looks from the results that ... (todo)

Keywords— LTE, Electromagnetic Radiation, power consumption, drones, femtocell, microstrip patch antenna, radiation pattern, specific absorption rate (SAR)

I. Introductie

THE Introduction in Dutch

II. Section

A. Gerelateerd werk

TODO

B. Scenario's

todo

C. Electromagnetische blootstelling

todo

III. Resultaten

todo

IV. Conclusie

todo

A. Referencies

todo

References

[1] Bart Lannoo, Didier Colle, Mario Pickavet, Piet Demeester, Optical Switching Architecture to Implement Moveable Cells in a Multimedia Train Environment, Proc. of ECOC 2004, 30th European Conf. on Optical Communication, vol. 3, pp. 344-345, Stockholm, Sweden, 5-9 Sep. 2004.

[2] Michael Neufeld, Ashish Jain, Dirk Grunwald, Nsclick:: bridging network simulation and deployment, http://systems.cs.colorado.edu/Networking/nsclick/

[3] The Click Modular Router Project, http://www.read.cs.ucla.edu/click/

[4] NS – Network Simulator, http://nsnam.isi.edu/nsnam/

Contents

List of Figures

List of Tables

List of Listings

Glossary

equivalent isotropic radiator A theoretical source of electromagnetic waves which radiates the same intensity for all directions. , 12, 13, 17, 25, 30, 38, 39, 44

power flux density Magnitude of power (W) that travels through a curtain area (m^2). , 18

RRP RRP is an abreviation used in this paper to indicate an extension on EIRP and stands for Real Radiation Pattern. An RRP value indicates the power (in dBm) for a certain location unlike an EIRP where the power (in dBm) is independent of the location. , 17

spurious radiation According to the thefreedictionary.com: Any emission from a radio transmitter at frequencies outside its frequency band. Also known as spurious emission. , 8

thermoregulatory capacity The capacity of an organism to regulate body temperture. , 5

Acronyms

D/L downlink. , 6, 7, 18, 24, 31, 34, 36, 39, 43

EIRP equivalent isotropic radiation power. , 11, 17, 34, 36, 50

Exp opt Exposure optimized.

FCC Federal Communications Commission. , 18

FDD Frequency Division Duplex. , 7

ICNIRP International Commission on Non-Ionizing Radiation Protection. , 4, 5

IEC International Electrotechnical Commission. , 18

LOS line of sigh. , 17, 35, 43

LTE Long-Term Evolution. , 7, 11, 18, 19, 29, 30

NLOS non line of sigh. , 35

PwrC opt Power consuption optimized.

SAR Specific Absorption Rate. , 5, 15, 16, 19, 31, 36, 39–44, 47, 48

TDD Time Division Duplex. , 7

U/L uplink. , 5–7, 16, 18, 19, 31, 40, 43, 44

UABS Unmanned Arial Base Station. , 3, 4, 6, 11–13, 15–18, 24–31, 33–36, 39–44, 46–50

UAV Unmanned Arial Vehicle.

UE User equipment. , 4, 11, 12, 16–19, 31, 36, 40, 42–44, 47, 50

WHIPP WiCa Heuristic Indoor Propagation Prediction.

1

Introduction

1.1 Outline of the Issue

Society is constantly getting more and more dependent on wireless communication. On any given moment, in any given location, an electronic device can request to connect to the bigger network. Devices need more than ever to be connected, starting from small IOT sensors up to self-driving cars which all need to be supported by the existing infrastructure. It is not surprising that the city center of Ghent has an average coverage of 97% of 4G over all telecom operators. [1]. Once again it becomes clear why we're on the eve of a new generation of cellular communication named 5G.

Also in exceptional and possibly life-threatening situations, the public relies on the cellular network. For example during the terrorist attacks at Brussels Airport, mobile network operators saw all telecommunications drastically increasing causing moments of contention. Some operators decided to temporarily exceed the exposure limits in order to handle all connections [2].

Electromagnetic exposure can however not be neglected. Research shows how excessive electromagnetic radiation can cause diverse biological side effects [3]. Because of public concern, the World Health Organization had launched a large, multidisciplinary research effort which

eventually concluded that there was no sufficient evidence that confirmed that exposure to low level electromagnetic fields is harmful [4]. A large part of the population remains nevertheless very concerned about potential health risks.

1.2 Objective

People are constantly getting exposed to several sources of electromagnetic radiation and it is important to consider this when designing a network. For this research, three prominent sources of radiation in a telecommunication network are investigated, being: the user's own phone, all base stations and all devices from other users in the network. In order to calculate electromagnetic exposure from all these sources, various parameters need to be known. Not only the used technology but also the position of the users and base stations are required. There are several publications discussing how the electromagnetic exposure originating from base stations can be calculated. Papers who cover electromagnetic exposure from all these different sources and convert it into a single value are rather limited.

To make this research possible, an existing planning tool is used which gives insight in user and base station distributions. The tool also provides information about path loss between radiators, power usage of the different electrical devices and which base station serves which user. In other words, the tool describes a fully configured network. In this way, all needed parameters will be known.

The electromagnetic behaviour of the network will be analysed by applying the tool in different scenarios to give insight which variables influence the exposure and how the network can be optimized accordingly. This leads to the following research questions:

1.3 Structure

Related research to the subject is discussed in chapter 2: State of the Art, explaining electromagnetic exposure and its absorption into the body. Also the used technology such as type of antenna, type of base station and which infrastructure will be examined. The chapter also discusses why this master dissertation differs from other papers. Thereafter, chapter 3 talks about the different scenarios that will be investigated. Eventually, the methodology covers in chapter 4 the calculations and implementation of the different aspects excerpted in State of the Art. Chapter 5 shows the results of this implementation for the scenarios described in chapter 3. Finally, a conclusion of these results is formed in chapter 6.

2

State of the Art

2.1 Deployment Tool for an UAV Network

Calculating electromagnetic exposure requires knowledge about the area. The position of base stations needs to be known, the transmission power used by the antenna and how far the user is separated from these base stations are only a few parameters that have to be considered.

The WAVES research group at UGent has developed a deployment tool for disaster scenarios with the aid of UAVs [5]. The idea of this UAV-aided emergency network is that in case of a disaster, the existing network might be damaged and won't be able to handle all users who are trying to reconnect to the backbone network. The tool makes a fast deployable network possible by attaching femtocells to UAVs, so-called UABSs. The tool will orchestrate the UABSs over the disaster area. This tool is thus a suitable starting point and works as follows:

The deployment tool will try to calculate the optimal placement for each UABS and requires therefore a description of the area where the UAV-aided network needs to be deployed. This is done with the use of so-called shape files. These files contain three dimensional descriptions of the buildings present in the area and are key values in approaching results as realistic as possible. Furthermore, the tool also requires a time period and a configuration file containing technical specifications of the type of UABS that is being used. The tool will thereafter ran-

domly distribute users over the area and assigns a certain bitrate to them.

In a second phase, the optimal position for each UABS is calculated. This is done by trying to locate a UABS above each active user. Two options are possible. If a fixed flying height is defined, a base station is placed above each user at the given height, unless a building is obstructing its location. Then, no base station will be located above that user. Alternatively to the fixed flying height, a flying margin can be defined which represents the distance between the outdoor user and the drone. If the user is inside, this margin will be measured between the drone and the rooftop of that building. The latter is only allowed if the suggested height remains below the given maximum allowed height.

Finally, all UABSs are sorted on whether they were active or not, followed by the increasing path loss from each UABS to that user. So the algorithm starts by checking for each active UABS if it can cover the user. If this is the case, the user will be connected to this UABS. If not, the second active base station with a (slightly) worse path loss is considered. If no active base station is suitable, inactive UABSs are considered. The user remains uncovered if no UABS is found. The reason behind only considering already active base stations at first, is the high cost that comes along with each drone.
Up till now, the tool has only calculated some suggestions. The actual provisioning is done in the fourth phase where drones are sorted by the amount of users they cover. As long as UABSs are available in the facility where they reside, UABSs are provisioned and its users are marked as covered.

2.2 Electromagnetic Exposure

2.2.1 Electromagnetic Field Radiation

People in a telecommunication network are exposed to far field electromagnetic radiation originating from base stations and other User equipment (UE). Network planners need to make sure that the electromagnetic fields (expressed in V/m) do not exceed limitations enforced by the government. These limits are location dependent. The European Union recommends the guidelines as defined by the International Commission on Non-Ionizing Radiation Protection (ICNIRP) which limits electromagnetic exposure to 61 V/m. Each European country needs to decide for themselves which limitations to enforce. Belgium for example delegated this responsibility to Flanders, Brussels and Wallonia [6].

The used deployment tool is applied in Ghent, a Flemish city in Belgium. The standards defined by the Flemish government are therefore applicable. They state that in the 2.6 GHz frequency

band, an individual antenna can't exceed 4.5 V/m and the cumulative sum of all fixed sources has its maximum at 31 V/m [6, 7].

2.2.2 Specific Absorption Rate

SAR represents the rate at which electromagnetic energy is absorbed by human tissue with the thermal effect as its most important health consequence. The volume of this tissue is typically 1 g or 10 g. The Federal Communications Commission of the United States defines regulations based on 1 g tissue (indicated as SAR_{1g}) while the European Union handles the 10 g model (SAR_{10g}). SAR values can further be categorized based on the area it covers. A first one is whole body SAR (SAR^{wb}) which is the average absorbed radiation over the entire body. The second type is more precisely. Localized SAR-values cover only a part of the human body like the head. The ICNIRP has concluded that the threshold effect for SAR^{wb}_{10g} is at 4 W/kg meaning that any higher absorption rate would overwhelm the thermoregulatory capacity of the human body. Whole body values between 1 and 4 W/kg increase the temperature of human body less than 1°C, which is proven not to be harmful for a healthy human being[8]. Thereafter, a safety margin is introduced to tackle unknown variables like experimental errors, increased sensitivity for certain population groups and so on. This results in a whole body SAR_{10g} of $0.8W/kg$ and $2W/kg$ for localized SAR_{10g} at head and torso area [6, 7].

2.2.3 Related Work

The goal of this master dissertation is the investigation of electromagnetic exposure considering all sources. Three types of sources are considered: electromagnetic radiation caused by base stations, near field radiation from the user's own device and far field radiation originating from other users' equipment. This electromagnetic radiation is thereafter absorbed by the human body which will be expressed in SAR values.

Several papers calculate exposure originating from certain sources, but very limited research has been done covering the whole picture. In [9] is described how electromagnetic radiation of several WiFi access points is being calculated. The authors of [10] used this knowledge to investigate electromagnetic exposure originating from base stations in a more outdoor environment. [11, 12] addresses the fact that also uplink (U/L) traffic from the user's device should be considered. They therefore investigated indoor exposure. They did not only consider the electromagnetic radiation but also how much is absorbed by the body, which will be expressed as specific absorption rate. Since the authors only covered voice calls, uplink SAR was expressed in localized SAR values while the downlink traffic is expressed in whole body SAR. With the advent of 5G, paper [13] has been published, describing how localized SAR values are achieved

from all sources. More precisely: all mobile phones and all base stations in the network after which they converted the electromagnetic exposure to localized SAR values. Finally, [14] describes how both U/L and downlink (D/L) traffic can be converted in whole body SAR values making it possible to achieve an overall picture. They applied this formula however only for the user's own device.

In a realistic network like the used deployment tool, some users are calling while others are using other types of telecommunication services like browsing the web. Therefore, all absorbed electromagnetic exposure should be expressed in whole body SAR while still covering all sources.

2.3 Optimizing towards Electromagnetic Exposure and Power Consumption

UABSs are drones with femtocell base stations attached to it. Drones can remain in the air for only a limited time, which is certainly the case when also an antenna needs to be connected to the battery of his carrier. It is therefore interesting to not only consider electromagnetic exposure of the user but also the power consumption that comes with it. However an increasing transmission power of an antenna comes with an increasing electromagnetic exposure. This is not the case considering both values for an entire network. In fact, the authors from [10] prove that both become inversely equivalent.

If a network is optimized towards power consumption, less drones will be provisioned radiating at higher power levels. This is because not only the transmission power is considered but also the power needed to keep the drone in the air. Therefore, it is cheaper to cover a user by increasing the antenna's transmission power of an already activated drone nearby as it therefore prevents the power cost of a new drone. By increasing the transmission power, also the electromagnetic exposure will increase for users closer to that drone. An exposure optimized network will therefore faster decide to power up a new drone.

2.4 Technologies

2.4.1 Type of Drone

Section 2.1 described how femtocell antennae will be connected to helicopter drones. Two types of drones are considered in [5]: an off-the-shelf drone affordable by the general public and a more expensive drone. The results in [5] show that the second type will require less drones to cover the same number of users and will last longer in the air. The research in this paper will

therefore be done with the usage of the second type. A technical overview of this drone is given in table 2.1.

Parameter	value
Carrier power	13.0 A
Average carrier speed	12.0 m/s
Average carrier power usage	17.33 Ah
Carrier battery voltage	22.2 V

Table 2.1: Specifications of the used drone.

2.4.2 LTE

The tool makes usage of Long-Term Evolution (LTE), by the general public better known as 4G. LTE allows better U/L and D/L data speeds compared to its predecessors and is based on an all IP architecture. This technology can cover macrocells supporting cell sizes ranging from 5 km up to 100 km. These types of antennae are usually attached to transmission towers along highways or on top of buildings. LTE supports however also smaller cells like femtocells covering only a few hundred meters. They are therefore more portable, require less energy and won't require a telecommunication operator because of their simplicity. Femtocell base stations are therefore used by the deployment tool. Further, LTE also support both Frequency Division Duplex (FDD) and Time Division Duplex (TDD).

FDD makes simultaneous U/L and D/L traffic possible by assigning different frequencies within the same frequency range to both data streams. A small guard band is used between the U/L and D/L direction in order to prevent interference.

TDD allows U/L and D/L traffic by splitting the time domain. Meaning that both traffic directions use the same frequency and therefore alternately (in time) use the same frequency. A small time interval is used to prevent interference in case of a slightly bad timed synchronization.

This master dissertation will make usage of FDD.

2.4.3 Type of Antenna

An important part of this master dissertation is the type of antenna that will be used by the femtocell base stations. The deployment tool makes use of drones that will position the femtocell base stations in the right position. Using conventional sector antennae, as used by traditional terrestrial transmission towers, would be too complicated for a simple drone. The characteristics of microstrip antennae will therefore be investigated.

Microstrip antennae provide several advantages compared to traditional antennae [**?**, 15]. Microstrip antennae are lightweight, low in cost and thin causing them to be more aerodynamic which is a useful feature since the antennae will be attached to flying drones.

A basic microstrip antenna like figure 2.1 consists of a ground plane and a radiating patch, both separated with a dielectric substrate. Several variations exist like microstrip patch antenna, microstrip slot antenna and printed dipole antenna which all have similar characteristics. They are all thin, support dual frequency operation and they all have the disadvantage that they will transmit at frequencies outside the aimed band which is also known as spurious radiation. The microstrip patch and slot antenna support both linear and circular polarization while the printed dipole only supports linear polarization. Further is the fabrication of a microstrip patch antenna considered to be the easiest of its competitors [**?**].

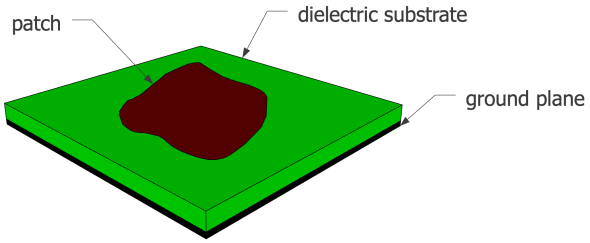

Figure 2.1: General design of a microstrip antenna.

The microstrip antenna requires besides the groundplane, dielectric substrate and the radiation patch also a feed line. Several feeding techniques exist of which the most popular are: coaxial probe feeding, microstrip line and aperture coupling.

A first feeding method is with the usage of a coaxial cable where the outer conductor is attached to the ground plane and the inner conductor to the radiations patch. Modelling is however difficult, especially for thick substrates as will be used in this master dissertation. A second option is the usage of a microstrip line. This type of feeding is much easier to model since the microstrip line can be seen as en extension of the radiating patch. A disadvantage is the increased spurious radiation which limits bandwidth. A third is proximity coupling which has the largest bandwidth and low spurious radiation. It consists however of two dielectric substrates causing the overall thickness of the antenna to increase as well as its fabrication difficulty [**?**].

The increasing usage of the microstrip patch antennae can be explained by it's easy fabrication and lightweightness and therefore knows a widespread application in the millitary, global possitioning systems, telemedicine, WiMax applications and so on. The authors of [16] also state that some of the disadvantages like lower gain and power handling can be solved with the usage of an array configuration.

The radiating patch is usually made of a thin layer of either gold or copper [15, 17] and can have any form. However, shapes other then circles or rectangles would require large numerical computation [15]. A simple rectangular shape will thus be used. Further, also the dielectric constant of the substrate is important. It typically varies between 2.2 and 12. Finding a good dielectric depends on how the antenna will used. A lower dielectric constant with a thick substrate will result in better performance, better efficiency and larger bandwidths [17]. On the other hand, a larger dielectric constant reduces de dimensions of the antenna [15] which is also useful when attaching the antenna to a limited surface. Glass as a dielectric substrate with a constant of 4.4 will be used.

3

Scenarios

The tool supports multiple configurations and the behaviour will be different for most these configurations. Three main scenarios will be investigated, order based on the network complexity. Within each scenario, different cases will be investigated. First, only one user with one drone will be present in the network. The network will thereafter be expanded for multiple users but with still only one drone available. Eventually, also that last restriction will be dropped meaning that multiple users with unlimited number of drones are examined. Table 3.1 shows the default values that are always applicable unless mentioned otherwise.

Broadband cellular network	
technology	LTE
frequency	2.6 GHz
Carrier	
carrier power	13.0 A
average carrier speed	12.0 m/s
average carrier power usage	17.33 Ah
carrier battery voltage	22.2 V
Femtocell antenna	
maximum P_{tx}	33 dBm
antenna direction	downwards (az: 0°; el: 90°)
gain	4 dBm
feeder loss	2 dBm
implementation loss	0 dBm
radiation pattern	EIRP or microstrip patch antenna
height	100m
UE Antenna	
height	1.5m from the floor
gain	0 dBm
feeder loss	0 dBm
radiation pattern	EIRP
number present in the network	224

Table 3.1: Overview of default configuration values.

3.1 A Single User

This first scenario will investigate how SAR_{10g} and power consumption behaves in an isolated environment meaning there is nor influence from other base stations nor other UE. The tool will provision one single drone and position it directly above the user. These results will however depend on the position of the user. If the randomly generated location of the user is indoor, the flying height of the drone might obstructed by the building where the user resides, causing the user to become uncovered. If this is not the case, the expected altitude of the user is half of the height of the building meaning that the user would be closer to the UABS as if he would have been outdoors. For more consistent results, the user will be positioned outdoor while systematically increasing the flying height.

Another considered variable will be the transmit power of the antenna. LTE makes usage of power control meaning that no more power will be used then strictly necessary. The actual

transmit power therefore ranges between 0 and the maximum input power. This power is zero when either no user is present or the user is so far away that the actual transmit power would exceed the maximum allowed transmission power. Increasing the maximum transmission power won't influence the actual power consumption or SAR_{10g} because the UABS won't use more then strictly required. It is therefore more useful to match the actual transmit power against a variable flying height.

This scenario investigates SAR_{10g}, power consumption and minimal transmission power for two different type of antennae: a fictional equivalent isotropic radiator and a realistic antenna. The used optimization strategy is not important for this scenario. This is because the decision algorithm decides which user needs to be connected to which drone. Since only one user and one UABS are available, both optimization strategies will behave identical.

The user gets a fixed position. The exact location doesn't matter as long as it is outside. For this experiment is chosen for the 'Koningin Maria Hendrikaplein', a square just next to the train station of Ghent. Doing so will force the UE to always be at the same height of 1.5 meters. An overview can be found in table 3.2

Parameter	**Value**
x position user	3.711198
y position user	51.036747
shadow margin user	-3.0398193
number of users	1

Input variables	**Output variables**
type of antenna	SAR_{10g}
flying height	power consumption
	minimal P_{tx}

Table 3.2: Overview of the configuration.

Note that there is no explicit restriction on the number of drones in table 3.2. The deployment tool initially places UABSs above each user and it is the optimization strategy that decides which of these potential positions remain in the end solution. Since there is only one user, there can also be only one drone.

3.2 Increasing Traffic with only one Drone available

This scenario investigates the same behaviour as the previous one. Still with only one drone but for a higher number of users. The scenario can be divided into two cases. The first case has a variable flying height with a fixed number of 224 users. This is the number of active users on an average day at 5 p.m. implying rush hour and therefore resulting in the highest number of simultaneous users for the day[5]. The other case has a fixed flying height of 100 m as recommended by [5] but with a variable number of users. To force the tool to only use one drone, a facility capacity is set to one indicating that there is only one spot available in the

facility where the UABSs are stored. The tool will still consider as much potential places as there are users in the network. But when the optimization algorithm is done, only one drone will remain.

Parameter	Value
facility capacity	1

Input variables	Output variables
type of antenna	SAR_{10g}
flying height	power consumption
number of users	user coverage
optimization strategy	

Table 3.3: Overview of the configuration.

For both cases, four configurations are possible because there are two antennae available (equivalent isotropic radiator and a realistic antenna) which can both operate in a power consumption optimized network or an exposure optimized network. The SAR_{10g}, power consumption and user coverage will be investigated for all four configurations.

3.3 Increasing Traffic with an Undefined Amount of Drones

Input variables	Output variables
type of antenna	SAR_{10g}
flying height	power consumption
number of users	user coverage
optimization strategy	

Table 3.4: Overview of the configuration.

The third scenario implies no budget limitations. The tool can use as much UABSs as desired while trying to maximize coverage. A UABS will be considered above each user which was also the case in scenario 2. However, the last step where the capacity of the facility was checked and drones got eliminates is omitted here. It is expected that the optimization strategies will perform best for this scenario since the decision algorithm has been written with multiple drones in mind. The scenario can once again be divided into two cases: one with a fixed flying height of 100 m and a variable number of users and a second one with a variable flying height and a fixed number of 224 users. The influence that these input parameters have on the network will be based on the electromagnetic exposure, power consumption, number of drones required and user coverage.

3.4 Overview

Three different scenarios will be investigated where the second and third one, each consist out of two cases. The first case is with a fixed flying height while the second one is with a fixed population size. Each case consist out of four configurations. An overview is given in table 3.1.

		Optimization strategy	
		Exposure optimized	Power consumption optimized
Antenna type	Equivalent isotropic radiator	EIRP, Exp opt	EIRP, PwrC opt
	Microstrip patch antenna	Microstrip, Exp opt	Microstrip, PwrC opt

Figure 3.1: Matrix with the four possible configurations

4

Methodology

4.1 Electromagnetic Exposure

4.1.1 Calculation of the Total Specific Absorption Rate

The total whole body SAR (SAR_{10g}^{wb}) of a user can be calculated by a simple sum of individual SAR values from the different sources. Formula 4.1 was originally described in [13] for SAR values induced into the head. Using SAR_{10g}^{head} would however result into incorrect conclusions since the position of the phone relative to the user is unknown. This is because the tool assigns a bitrate to a user depending on the service he is using meaning that users in the network are not only calling but are able of using other services as well like browsing the web. The position of the phone can thus be next to the head but also in front of the user. The induced electromagnetic radiation will therefore be expressed in function of the entire body.

$$SAR_{10g}^{wb,total} = SAR_{10g}^{wb,ul} + SAR_{10g}^{wb,dl} + SAR_{10g}^{wb,neighbours} \tag{4.1}$$

The first parameter, $SAR_{10g}^{wb,ul}$, will indicate the absorbed electromagnetic radiation by the whole body originating from the user's own device. However that the radiation is destined for the serving UABS, a portion of that radiation is directly absorbed by its user. The second

parameter $SAR_{10g}^{wb,dl}$ will represent the absorbed electromagnetic radiation caused by all the femtocell base stations in the considered area. The last factor, $SAR_{10g}^{wb,neighbours}$, specifies the exposure of our user to U/L radiation from other mobile devices. An illustration is given in figure 4.1 where red and yellow are types of far field radiation and green near field radiation. This is further explained is subsequent chapters along with how each value in this formula can be calculated.

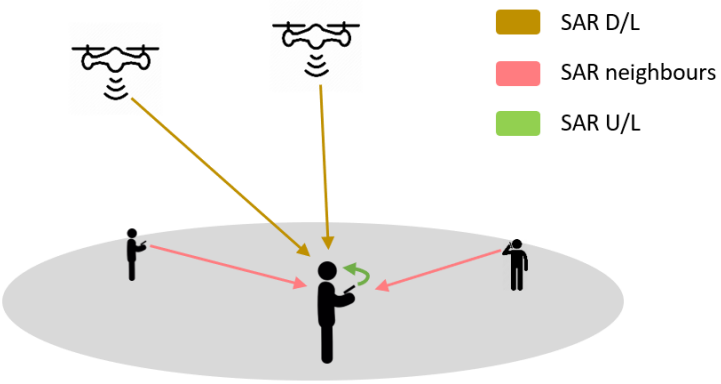

Figure 4.1: Illustration of the network that shows how the average user (here shown in the center) is influenced by different type of sources. We can only speak in terms of SAR when the electromagnetic radiation is absorbed by the user. This last step is however not shown in the illustration.

4.1.2 Electromagnetic Exposure Caused by Far-Field Radiation

The electromagnetic exposure to which people are exposed can be categorized in two groups. One of them is near-field radiation which is caused by the user's own device and which will be discussed in 4.1.3. The other type is far-field radiation and will be explained in this section. This kind of radiation is caused by radiators 'far away'. Examples of these types of radiators are UE which belong to other people and UABSs.

Electromagnetic Radiation from a Single Source

To determine the total exposure of a single human being or even of the entire network, the electric-field $\vec{E}$ from a single radiator i should be calculated. The formula to determine this electromagnetic value E (expressed in V/m) for a specific location u is given in equation 4.2.

$$E_i(u) = 10^{\frac{RRP(u)-43.15+20*\log(f)-PL(u)}{20}} \tag{4.2}$$

frequency The used frequency in the formula above is denoted as f and is expressed in MHz. Since LTE is used, this value will be 2600 MHz.

Real Radiation Power and EIRP In formula 4.2, as it was described in [9, 10], RRP was defined as equivalent isotropic radiation power (EIRP). EIRP is the radiation generated by an equivalent isotropic radiator which is a theoretical source of electromagnetic waves that radiate with the same intensity in all directions. The formula to find this EIRP value (in dBm) is described in 4.3 where P_t stands for the input power of the antenna, G_t for the gain of the transmitter and L_t being its feeder loss.

$$EIRP = P_t + G_t - L_t \tag{4.3}$$

This formula, which is constructed out of different gains and losses, misses a factor when accounting for real life radiation patterns. Formula 4.2 solves this by using RRP instead of EIRP which can be defined as follows:

$$RRP(u) = EIRP - attenuation(u) \tag{4.4}$$

The attenuation for a user u is given based on the angle between the main beam and the user. More details on how this can be implemented is described in 4.3.2. When assuming that $attenuation(u)$ returns positive values, the attenuation can simply be subtracted from the EIRP-value.

path loss At last, formula 4.3 requires the path loss (in dB). In order to calculate this, an appropriate propagation model -of which several exist- is required . The tool uses the Walfish-Ikegami model because it performs well for femtocell networks in urban areas [5]. The chosen propagation model consists of two formulas depending on whether a free line of sigh (LOS) between the user and the base station exists or not. Both formulas expect a distance in kilometre.

Combining Exposure

The electromagnetic exposure for a given location originating from different sources can be calculated with formula 4.5 (in V/m). E_i stands for the electromagnetic exposure from source i and n stands for all far-field radiators of a certain category which will either be UABSs or UE from other people. E_{tot} was originally calculated for each x meters [10]. In the tool, the exact location of the users is known and E_{tot} will thus only be calculated for locations where a user is positioned.

$$E_{tot} = \sqrt{\sum_{i=1}^{n} E_i^2} \tag{4.5}$$

Converting Far-Field Electromagnetic Exposure to SAR_{10g}^{wb}

Formula 4.1 expects that the electromagnetic radiation is expressed into $SAR_{10g}^{wb,dl}$ and $SAR_{10g}^{wb,neighbours}$. The calculation for both values is in fact identical. The only difference is the source; where the first one is for UABSs, the second one for UE. Physically seen, they are both whole body SAR values induced by far-field radiation ($SAR_{10g}^{ff,wb}$).

The electromagnetic radiation needs to be converted into $SAR_{10g}^{ff,wb}$. This conversion factor is based on Duke from the Virtual Family. Duke is a 34-year old male with a weight of 72 kg, a height of 1.74 m and body mass index of 23.1 kg/m [14]. Research shows that the conversion factor for WiFi is $0.0028\frac{W/kg}{W/m^2}$. Since WiFi, at a frequency of 2400 MHz, is very close to LTE, at 2600 MHz, it is assumed in [14] that this value is also applicable for LTE. This constant converts the power flux density S (with units $\frac{W}{m^2}$) to the required $SAR_{10g}^{ff,wb}$. To make this possible, the electromagnetic radiation from formula 4.5 (expressed in V/m) should first be converted to the power flux density with formula 4.6 before formula 4.7 can be applied.

$$S = \frac{(E_{tot})^2}{337} \tag{4.6}$$

$$SAR_{10g}^{wb,ff} = S * 0.0028 \tag{4.7}$$

4.1.3 Electromagnetic Exposure Caused by Near-Field Radiation

When a user is operating his device, a part of the U/L radiation will enter his body despite the fact that the traffic is destined for the serving UABS. So the electromagnetic exposure won't be limited by D/L traffic from UABSs or U/L traffic from other UE but also from U/L traffic from his own device.

Localized Specific Absorption Rate

When assuming that all users hold their device next to their ear, a localized SAR-value for the head SAR_{10g}^{head} can be calculated. Various governments have defined different legislations. The European Union uses the directions of the IEC who define in IEC:62209-2 a maximum for a 10g tissue SAR_{10g}^{head} as 2 W/kg [6]. The FCC limits the maximum in the United States for a 1g tissue SAR_{1g}^{head} at 1.6 W/kg [18]. Most countries, including Belgium, enforce the 10g model and will, therefore, be the point of reference for this master dissertation. The SAR_{10g}^{head} values are phone dependent. The values reported by mobile manufactures are worst-case scenarios meaning that the values are measured when the phone is transmitting at maximum power. This is an

understandable decision but won't result in a realistic scenario since modern cellular networks use power control mechanisms to prevent unnecessary high radiation of a nearby device. UE will therefore never use more energy than required to maintain a connection. To compensate for this overestimation, the actual SAR_{10g}^{head} of each user will be predicted. These will, however, remain an estimation since the position of the phone relative to the head differs from user to user. For example, by holding the phone differently, a hand can absorb more or less electromagnetic radiation. The SAR values will also depend on the age of the user, especially children who experience on average higher exposure in the brain regions because of different anatomical proportions [19, 11].

$$SAR_{10g} = \frac{P_{tx}}{P_{tx}^{max}} * SAR_{10g}^{max} \tag{4.8}$$

Equation 4.8 will be used to predict the actual SAR_{10g}^{head} of a certain user with P_{Tx}^{max} being the maximum transmission power for a phone which is in LTE and UMTS 23 dBm [20, 11]. The actual transmitted power (P_{tx}) is calculated with equation 4.9 where P_{sens} stands for the receiver sensitivity and PL the path loss between sender and receiver.

$$P_{tx} = P_{sens} + PL \tag{4.9}$$

However the legal SAR_{10g}^{max} for Belgium is set to $2W/kg$, the actual SAR_{10g}^{max} value is usually lower and different for each mobile device. An average is calculated based on 3516 different phones from various brands using a German database [21] for which an overview can be found in fig. 4.2. When the phone is positioned at the ear, an average of 0.7 W/kg is found with a standard deviation of 0.25 W/kg which are very similar results as in ref. [22]. The median of 0.67 W/kg is used.

Whole body Specific Absorption Rate

The position of the phone relative to the user's body is however unknown. The tool assigns different bitrates to different phones implying that some users are calling and therefore probably holding their phone next to their ear while another part is using other services like browsing the web. For this reason formula 4.1 expects that the specific absorption rate is expressed for the entire body instead of localized SAR_{10g}^{head}. The conversion factors for Duke from the Virtual Family will be used again as it was already the case in 4.1.2. The constant to convert U/L exposure to $SAR_{10g}^{wb,ul}$ for WiFi is defined to be 0.0070 $\left(\frac{W/kg}{W}\right)$ [14] which leads to eq. 4.10.

$$SAR_{10g}^{wb,ul}\left(\frac{W}{kg}\right) = 0.0070\left(\frac{W/kg}{W}\right) * P_{tx}(W) \tag{4.10}$$

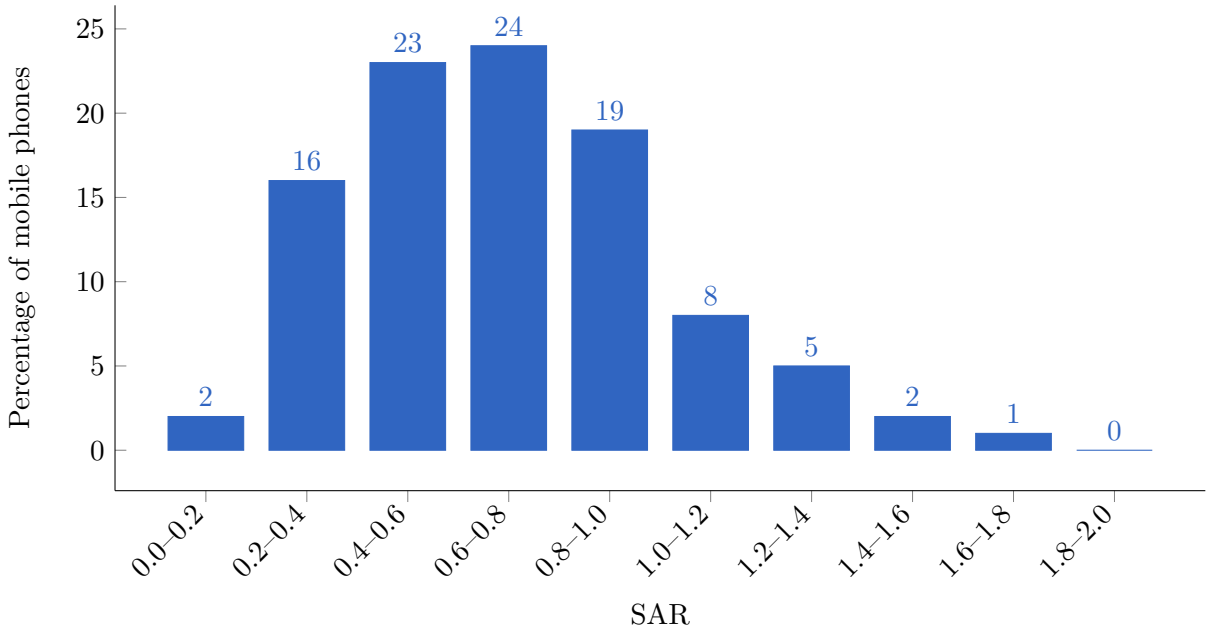

Figure 4.2: Distribution of how many phones belong to a certain SAR interval. Upper boundary not included.

4.1.4 Defining an Antenna

A microstrip patch antenna is chosen because it allows easy production but more important, it has a low weight and has a thin profile causing it to be very aerodynamic which is useful when attaching it to a drone [16].

The dimensions of the antenna depend on the frequency it is operating at and the characteristics of the used substrate. The antenna will be radiating at a center frequency f_0 of 2.6 GHz. Each substrate has a dielectric constant ϵ_r representing the permittivity of the substrate and depends on the used material. Substrates with a high dielectric constant and low height reduce the dimensions of the antenna while a lower dielectric constant with a high height improves antenna performance. In this paper, a substrate like glass is chosen because of the higher dielectric constant of $\epsilon_r = 4.4$ compared to materials like teflon with only a dielectric constant of $\epsilon_r = 2.2$ [15]. Doing this in combination with an antenna height of 2.87 mm will decrease the dimensions of the entire antenna surface. This comes in handy since drones only have limited space available.

description	symbol	value
center frequency	f_0	2600 Hz
dielectric constant	ϵ_r	4.4
heigt of the substrate	h	0.00287 m

Table 4.1: Overview of configuration parameters.

The dimensions of the radiating patch can be calculated with the formulas from [15] and [17] using the defined values from table 4.1. In that way, the width W is calculated using formula 4.11.

$$W = \frac{C}{2 * f_0 * \sqrt{\frac{\epsilon_r + 1}{2}}} \tag{4.11}$$

With C being the speed of light, f_0 the center frequency of 2600 MHz and a dielectric constant ϵ_r of 4.4. This results in a width of 3.51 mm.

In order to find the length of the radiating patch, some other values need to be determined first. Formula 4.12 will calculate the effective dielectric constant (ϵ_{reff}).

$$\epsilon_{reff} = \frac{\epsilon_r + 1}{2} + \frac{\epsilon_r - 1}{2} * \left(1 + 12 * \frac{h}{W}\right)^{-\frac{1}{2}} \tag{4.12}$$

This formula requires the width found in the previous formula along with the dielectric constant and substrate height from table 4.1. This will result in a ϵ_{reff} of 3.91.

$$L_{eff} = \frac{c}{2 * f * \sqrt{\epsilon_{reff}}} \tag{4.13}$$

Now formula 4.13 can be used to calculate effective length (L_{eff}) which results in 29.16 mm.

$$\Delta L = 0.412 * h * \frac{(\epsilon_{reff} + 0.3)\left(\frac{W}{h} + 0.264\right)}{(\epsilon_{reff} - 0.258)\left(\frac{W}{h} + 0.8\right)} \tag{4.14}$$

Eventually, the length extension is found with formula 4.14 by substituting the values from above. Doing so determines that the ΔL equals 1.3071 mm.

Finally, the length of the patch can be calculated using the expression: $L = L_{eff} - 2 * \Delta L$ which results in 26.55 mm.

The dimensions of the radiation patch are now known. The only remaining questions are the dimensions of the ground plane and dielectric substrate to which the radiation patch is attached. The transmission line model is in fact only applicable for an infinite ground plane but it has been proven that similar results can be achieved if the ground plane's dimensions are bigger than the patch by approximately 6 times the height of the dielectric substrate [15, 17].

$$L_g = 6 * h + L \tag{4.15}$$

$$W_g = 6 * h + W \tag{4.16}$$

Therefore, the length of the ground plane L_g should be at least 0.0438 m and a width W_g at least 0.0524 m. A schematic overview of how the antenna will look like is given in figure 4.3.

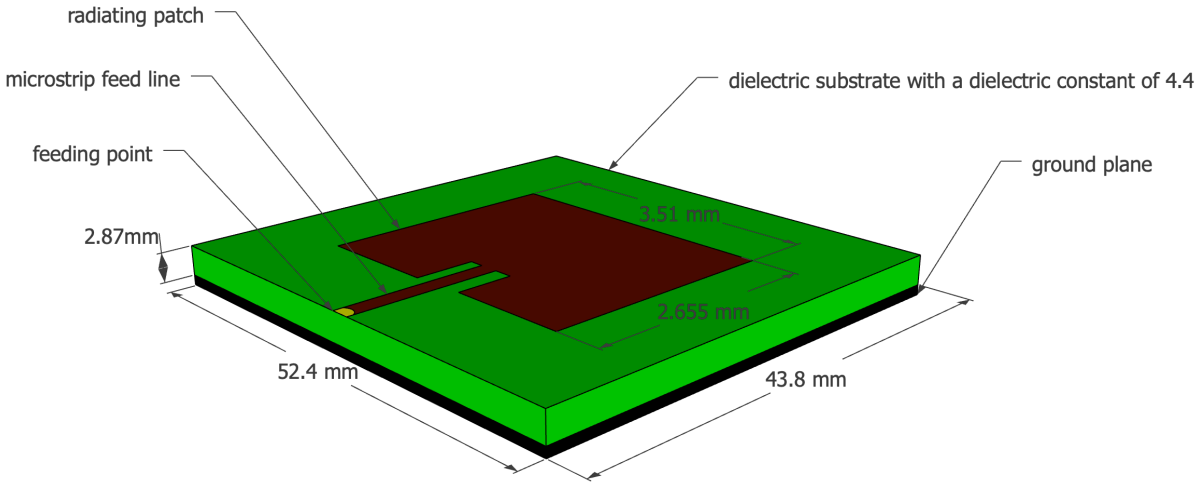

Figure 4.3: Design of the microstrip patch antenna.

4.1.5 Radiation Pattern

Mathlab is able to generate the radiation pattern for this microstrip patch antenna. The code in listing 1 starts by defining the dielectric substrate which will be glass with a dielectric constant of 4.4 and a height of 0.00287 m. Thereafter, the microstrip patch antenna is generated with the `width` and `length` being the dimensions of the radiation patch and the `GroundPlaneLength` and `GroundPlaneWidth` the dimensions of the ground plane and dielectric substrate. The `FeedOffset` is the relative offset from the center where the radio frequency power is fed to the radiating patch which will here be at the edge. This is in figure 4.3 indicated with the yellow dot. At last, the `dielectric`-object is substituted into the `patchMicrostripInsetfed`-object.

Generating the pattern is done with the `pattern`-command. The first value is the `patchMicrostripInsetfed`-object followed by the frequency at which the antenna will be operating. Optionally, an azimuth value can be parsed like in line 7 and 8 where 90 and 0 relatively stand for the H-plane and E-plane.

Running the configuration from listing 1 will generate the radiation pattern from figure 4.4. When running the same configuration for a slightly bigger square ground plane with an edge of 0.060 m, the radiation pattern from 4.5 is achieved. Both radiation patterns show an aperture angle of approximately 90°. It becomes clear that the radiation pattern from figure 4.4 has a higher attenuation in the direction it is not facing compared to the radiation pattern of figure 4.5. If it is assumed that drones fly lower than some users are positioned in some buildings,

```
d = dielectric("Name",'glass',"Thickness",0.00287,"EpsilonR",4.4)
p = patchMicrostripInsetfed("Width",0.0351,"Length",0.02655,
    "GroundPlaneLength",0.0438,"GroundPlaneWidth",0.0524,
    "FeedOffset",[-0.021885 0],"Substrate", d)

pattern(p,2.6e9, "CoordinateSystem", 'polar', "Normalize",true)
pattern(p,2.6e9, 90, "CoordinateSystem", 'polar', "Normalize",true)
pattern(p,2.6e9, 0, "CoordinateSystem", 'polar', "Normalize",true)
```

Listing 1: Mathlab code to generate radiation pattern for a microstrip patch antenna.

the pattern of 4.5 would be a better approach. However, for the continuation of this master dissertation, the radiation pattern from figure 4.4 will be used since this antenna is the smallest and therefore more suitable to attach to the limited space available under a drone. A data sheet of the exact values from both radiation patterns can be found in appendix A.

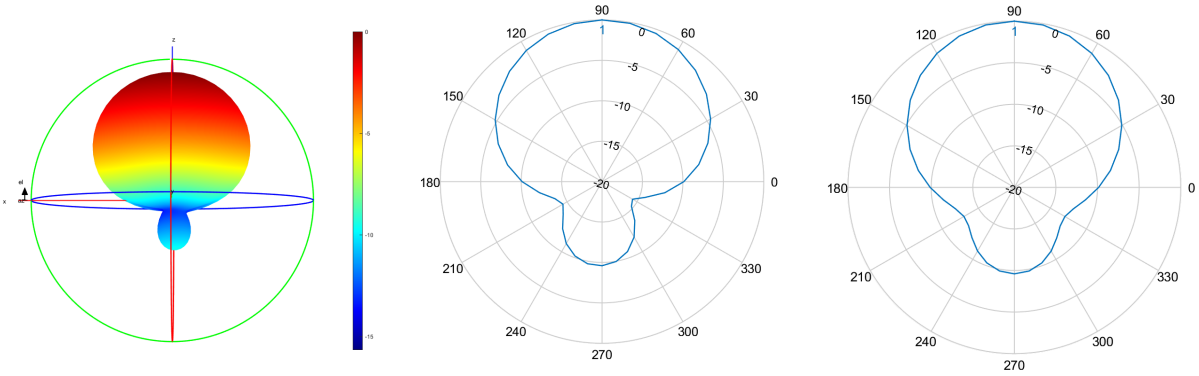

Figure 4.4: Radiation pattern 1: On the left a 3D model of the entire pattern with the configuration as described above. In the middle a 2D radiation pattern of the E-plane and at the right a 2D model of the H-plane.

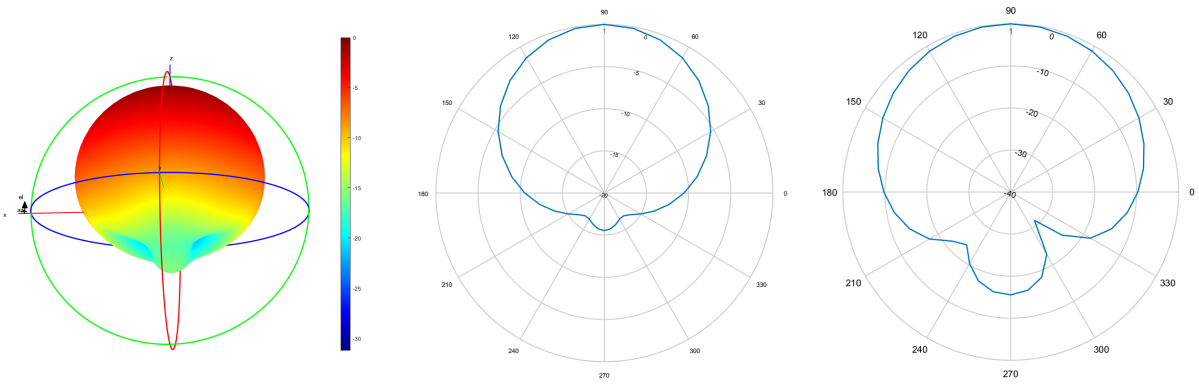

Figure 4.5: Radiation pattern 2: Generated with a groundplane of 0.06m by 0.06m. On the left is the 3D model of the entire pattern plotted. In the middle a 2D radiation pattern of the E-plane and at the right a 2D model of the H-plane.

4.2 Optimizing the Network

The network, as originally defined in the deployment tool, tried to minimize power consumption by connecting the user to a base station which experienced the lowest path loss. A second optimization strategy is introduced, based on the fitness function described in [10].

$$f = w * \left(1 - \frac{E_m}{E_{max}}\right) + (1 - w) * \left(1 - \frac{P}{P_{max}}\right) * 100 \tag{4.17}$$

Formula 4.17 returns a fitness value which represents the performance of the entire network. Users are connected to different UABSs and each time a fitness value is calculated. The user will eventually be connected to the drone resulting in the highest fitness value. This process is repeated for each user. w is the importance factor of electromagnetic exposure ranging from 0 to 1, boundaries included. A w set to zero means that electromagnetic exposure is not important. Such a network will therefore be called a power consumption optimized network. Likewise, a w set to one means that minimizing exposure is top priority and will result in an exposure optimized network. P_{max} is the power consumption of all UABSs, both active and inactive, when radiating at the highest possible level while P is the effective power used by the current designed network. This will be the power required for the flying drones themselves and their antenna. E_m will be the weighted exposure of the average user for the current designed network and E_{max} the weighted average electromagnetic exposure when all antennae are at their highest power level.

When optimizing the network, it is not only important to consider the average exposure of all users, but also to limit high extremes [10]. A weighted average will be used not only considering the median but also the 95 percentile from all users' D/L exposure using formula 4.18. Since

both values are considered to have equal importance, the weight factors w_1 and w_2 will both have an equal importance of 50%.

$$E_m = \frac{w_1 * E_{50} + w_2 * E_{95}}{w_1 + w_2} \tag{4.18}$$

4.3 Implementation

4.3.1 Network Planning, Bringing It All Together

The existing algorithm as described in section 2.1 is extended to support different optimization strategies by using the formulas from section 4.2. As explained in State of the Art, the program starts with the preparation of the network by distributing the users over the network and assigns the bitrate required for each user's cell phone activity. Thereafter, the tool tries to solve this network by assigning a UABS above each user. This master dissertation will only cover fixed flying heights meaning that a certain position is only infeasible if it is obstructed by a building.

Solving the network starts by calculating the path loss between all users and between users and UABSs. Thereafter, the tool iterates over each user and tries to connect that user to each UABS. This connection is not always possible. A UABS might be saturated with users and won't be able to cover yet another user or maybe the user is so far away that in order to cover that user, the UABS would exceed its maximum allowed input power. If however a connection is possible, the user will be connected to that UABS and the fitness function from section 4.2 is used. Only the connection which results in the best fitness value for the entire network will be used. Thereafter, the tool shifts to the next user.

Up till now, the tool assumed an unlimited number of drones but this is an unrealistic scenario. Certainly when high number of users are present in the network. The number of available drones can be limited by defining the capacity of the facility where the drones are stored. If such a capacity is defined and the number of active drones exceed this limitation, the tool will delete the necessary drones starting by those who cover the least number of users. These users will now become uncovered.

4.3.2 Implementation of the Radiation Pattern

The deployment tool originally only supported equivalent isotropic radiators. The tool has thus been extended and is fully configurable allowing any possible antenna in any possible orientation with the usage of a XML-file. The configuration described in this file will apply to all UABSs.

The orientation is done using two values called ‘downtilt’ and ‘north offset’. The first value defines the downtilt angle under wich the antenna is pointing. A downtilt angle of zero degrees is perfectly horizontal and an antenna with a downtilt angle of 90° will be pointing straight to the ground. This parameter only supports positive values ranging from 0° to 360° (upper boundary not included). An antenna pointing to the sky would therefore require a value of 270°. The second value, the north offset, defines the azimuth orientation of the drone. The value given to this parameter indicates the offset between the north and the horizontal direction to which the antenna should be pointing at. The value once again ranges from 0° to 360° with the upper boundary not included. The angle is calculated in counterclockwise orientation. For instance, a north offset of 270° will let the UABS point to the east.

Thereafter, the normalized radiation pattern is supplied to the tool. The actual pattern is three dimensional. To simplify this, slices perpendicular to the az-axis are extracted. These are indicated in figure 4.6 with azimuth cuts. With an angle of 90° four slices are achieved, each consisting out of elevation cuts. The intersection of an elevation and azimuth plane corresponds with a certain attenuation which is fed to the tool. Figure 4.6 shows only 3 elevation planes. The radiation pattern used in the tool has an attenuation every 10°. In other words, a slice consists of 19 values ranging from 0° to 180° (boundaries included).

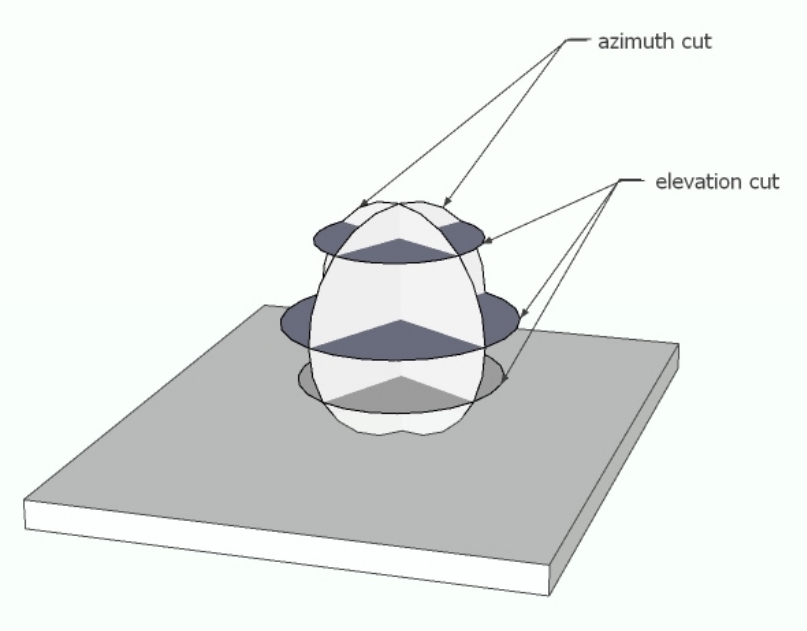

Figure 4.6: Schematic example of slices in a radiation pattern.

The number of required slices depends on the complexity of the radiation pattern. For symmetrical radiation patterns, like in figure 4.4 and 4.5, two azimuth cuts perpendicular to each other dividing the radiation pattern in 4 azimuth-slices are definitely sufficient. However, this might

not be the case for radiation patterns with a more complex structure containing several side lobs. To tackle this issue, more azimuth-slices can be defined for increased precision. Each slice should however contain an equal amount of elevation slices. A concrete example of a configuration file can be found in appendix B.

When the attenuation of a user from a certain UABS needs to be known, the elevation and azimuth angles between the user and the antenna's direction should be calculated. Figure 4.7 represents a radiation pattern with the black dot indicating the user whose attenuation needs to be calculated. The small black lines represent azimuth and elevation planes. The tool knows the exact attenuation only at the intersection of those lines. The chance that a user is positioned at such an intersection is very small. Therefore, the attenuation for the requested point has to be estimated using bilinear interpolation. First, the attenuation is estimated at the intersection of the red and orange line using linear interpolation on the horizontal axis with the known values at the end of the red line. The same is done for the orange-green intersection using the known values at the end of the green line. Finally, linear interpolation is applied to the y-axis for the black dot on the orange line using the estimated values at the end of the orange line.

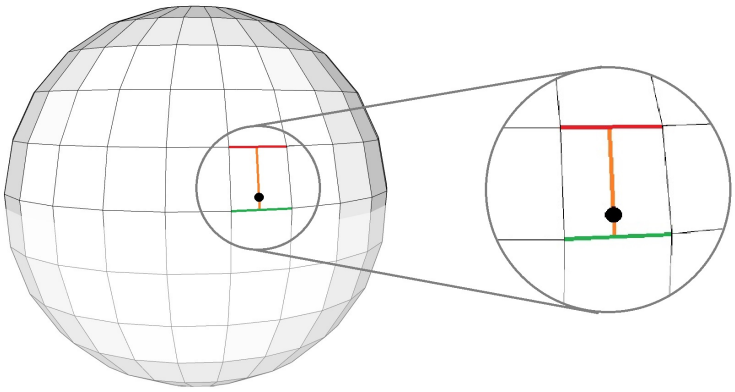

Figure 4.7: Schematic example of how bilinear interpolation works.

4.3.3 Performance Improvement

Calculating Path Loss

The path loss is required by several formulas. For instance, the formula that decides whether a UABS is feasible for a certain user makes usage of this parameter but also the calculations for the downlink electromagnetic exposure require this value to be known. The formulas for the whole body SAR_{10g} require not only the path loss between the user and all UABSs but even the path loss between users themselves. These path loss calculations are based on the Walfish-Ikegami model that causes a high computational load. The calculation between two points is

completely independent of any other calculation between any other points and is therefore a suitable candidate to multithread. The deployment tool creates two thread pools. The first pool creates a thread for each user where each thread calculates the path loss between the user assigned to him and all possible UABSs, causing a time complexity of n^2. Each user stores all path losses between himself and any other UABS. This results therefore in a total space complexity of n^2. When all users are finished, the thread pool is shut down and the second one is created for the same calculations but between users. The pool will, just like the previous, create threads for each user but there is an important difference. When a certain user calculates the path loss to another user, this path loss also applies for the other direction. The tool saves time by calculating the path loss only once and stores the path loss at both users. It is therefore sufficient that a given user only calculates path losses of users at his right side, since the other path losses will be calculated by the users on his left. This results in a time complexity of only $n(\frac{n}{2})$. When the last user finishes his thread, all users know the path loss of all other users causing a space complexity of $n(n-1)$.

Limiting Antenna Searching

The user needs to be connected to the 'best' base station. To identify this best UABS, the user should be connected to each base station and the fitness value 4.17 of the network has to be evaluated. The connection that resulted in the best fitness function will be added to the solution. This process is repeated for each user but can further be improved. A user will likely be connected to either the UABS directly above him or to a UABS in the direct neighbourhood. Time complexity can thus be improved by not considering drones outside a certain radius. An ideal data structure for neighbourhood-search is a KD-tree. This data structure is based on a binary tree and is optimal for objects with multiple keys. Objects are thus positioned in K dimensions where each node splits the hyperplane over exact one dimension. The dimension that needs to be split depends on the level of the KD-tree in which that node is situated. In this case, the x and y coordinate will be used in a 2D-tree (k=2) like in figure 4.8.

In this case the choice was made to only consider UABSs within a radius of half a kilometre. This will result in 23 UABSs on average when applied to a default scenario of 224 UABSs at a flying altitude of 100 m.

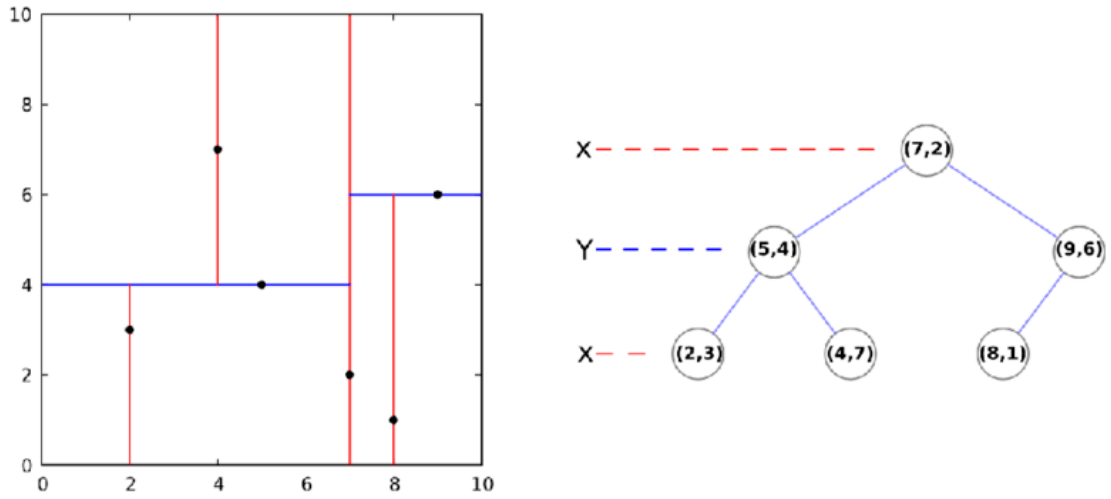

Figure 4.8: Example of a KD-tree in two dimensions.

5

Results and Discussion

5.1 Scenario 1: One User and One Drone

The network contains only one user for this scenario. This means that there is only one location possible for the drone which is just above the user. This section will investigate minimal required transmission power and SAR values from different sources. power consumption te doen

5.1.1 The Influence of the Maximum Transmission Power

LTE makes usages of power control meaning that no more power will be used then strictly necessary. The actual transmit power P_{tx} therefore ranges between zero and the maximum allowed input power. P_{tx} is zero when the UABS doesn't cover anybody. For instance when the flying height is too high and therefore also the path loss that comes with it, the maximum allowed P_{tx} is not enough to cover the distance. In such case, the UABS is shut down since it cannot meet the requirements. Increasing the maximum transmission power won't influence the actual used P_{tx} or SAR_{10g} because the UABS won't use more then strictly required. It is therefore more useful to match the actual transmission power against a variable flying height.

Figure 5.3 shows the logarithmic relationship between P_{tx} and flying height. As already discussed

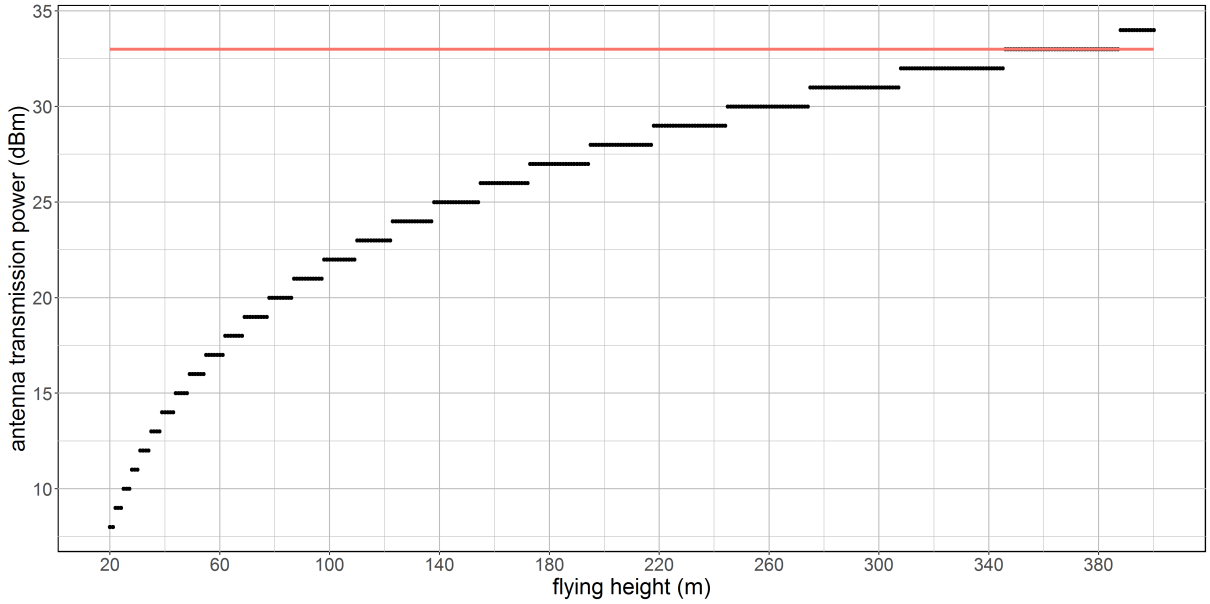

Figure 5.1: Minimal required transmission power by the antenna to reach the ground just below him. The red line shows the default maximum transmission power.

in 3.1, the user is outdoor and just below the UABS. There is thus a free line-of-sight between both radiators. It is clear from figure 5.3 that a discontinue step function is achieved. This is because multiple flying heights correspond to the same transmission power. When the flying height increases, so does the path loss. LTE tries to counteract this by increasing the power level. Each time the path loss becomes too high, the power level of the antenna increases with one dBm. Doing so, decreases path loss allowing the antenna to reach the user again.

After a jump in the step function, there is an overestimation meaning the input power increased more then necessary. So multiple flying heights correspond with the same P_{tx}. Further, dBm is also a logarithmic scale meaning that while 10 dBm equals 10 mW, 20 dBm equals 100 mW. This explains why the black lines become longer at higher flying altitudes. Each time the power level increases with one dBm, the overestimation becomes larger. If the tool would make usage of a smaller step size, a more continuous logarithmic function would be achieved. This would however worsen the time complexity because it would take much more iterations before the power level exceeds the path loss.

The red line in figure 5.3 indicates the default maximum transmission power used during simulations. In a free line-of-sight scenario with only one user, a UABS can fly up to 387 metres before losing connection.

This scenario is investigated with a microstrip patch antenna using power consumption optimization. The configuration, however, does not matter despite the fact that an equivalent isotropic

radiator doesn't have any attenuation while a microstrip patch antenna does. Since the user is positioned in the perfect center of the main beam where there is no attenuation experienced in either cases. Also the optimization won't make a difference. The goal of the optimization strategy is to decide which drone is most suitable for which users. Since there is only one user and one possible position for the drone, both optimization strategies behave identical.

5.1.2 Influence of the Flying Height

This section investigates how the flying height of a UABS influence SAR_{10g} and power consumption. This induced electromagnetic radiation for our user is represented in figure 5.2 and shows that for low flying drones, UABSs are the main source of electromagnetic radiation (green line). This changes around 80 meters where the U/L electromagnetic radiation of the UE (red line) exceeds the D/L radiation in order to still be able to reach the high flying UABSs.

SAR-values are caused by the input power of the antenna. The P_{tx} in section 5.1.1 showed a discontinue behaviour that sometimes radiate more as strictly necessary. This has thus a direct influence on SAR^{dl}_{10g}. Hence the same discontinue behaviour. SAR^{dl}_{10g} can be simplified to an perfect constant line. This constant behaviour can once again be explained with power control. When the UABS flies lower, there is less path loss and the UABS will therefore reduce the P_{tx}. This results in formula 5.1 where the electromagnetic exposure is a constant fraction of power and distance.

$$\vec{E}(V/m) = \frac{\Delta U(V)}{\Delta x(m)} \tag{5.1}$$

Figure 5.2 doesn't show radiation from neighbours, because there are none present in this scenario. Finally, all these values are added as explained in formula 4.1 and indicated with the blue line.

power consumption te doen

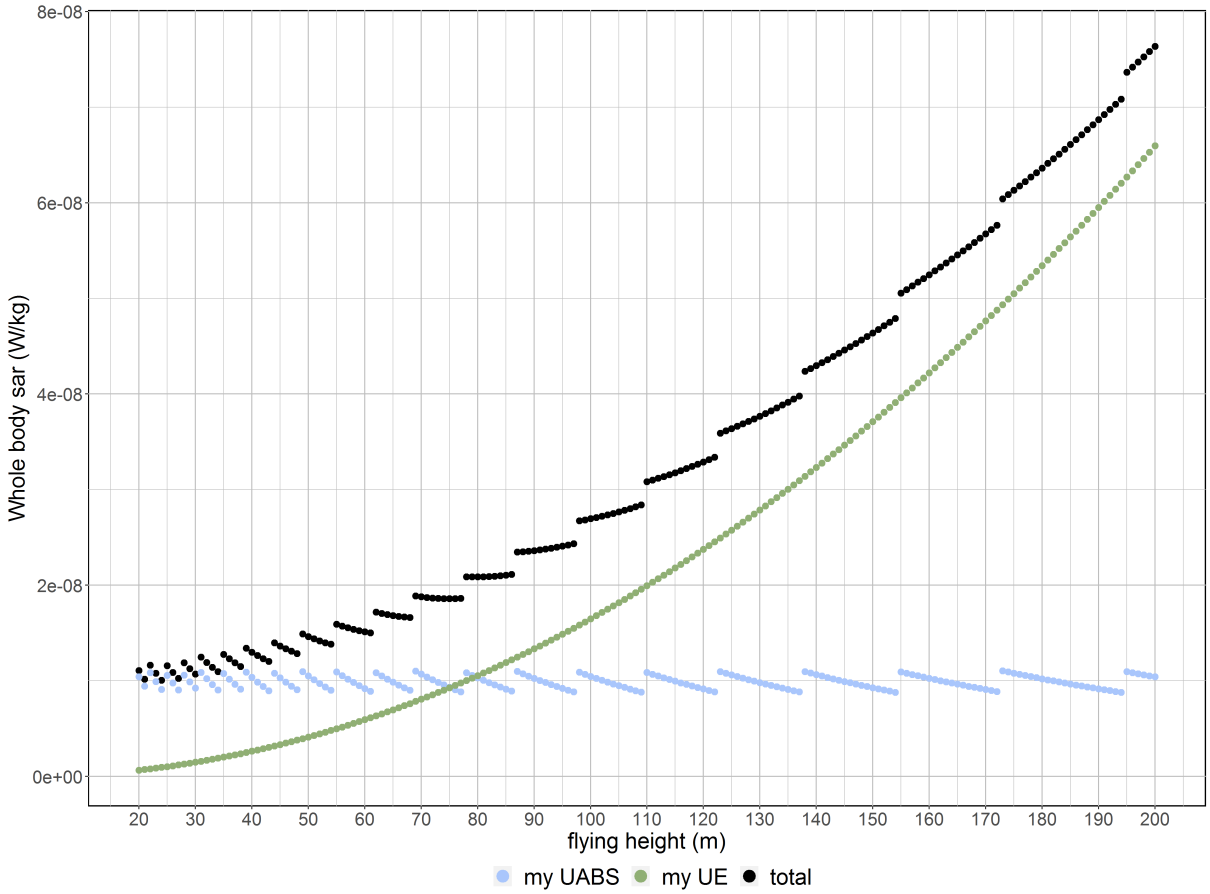

Figure 5.2: How SAR values from different sources are influenced by different flying altitudes.

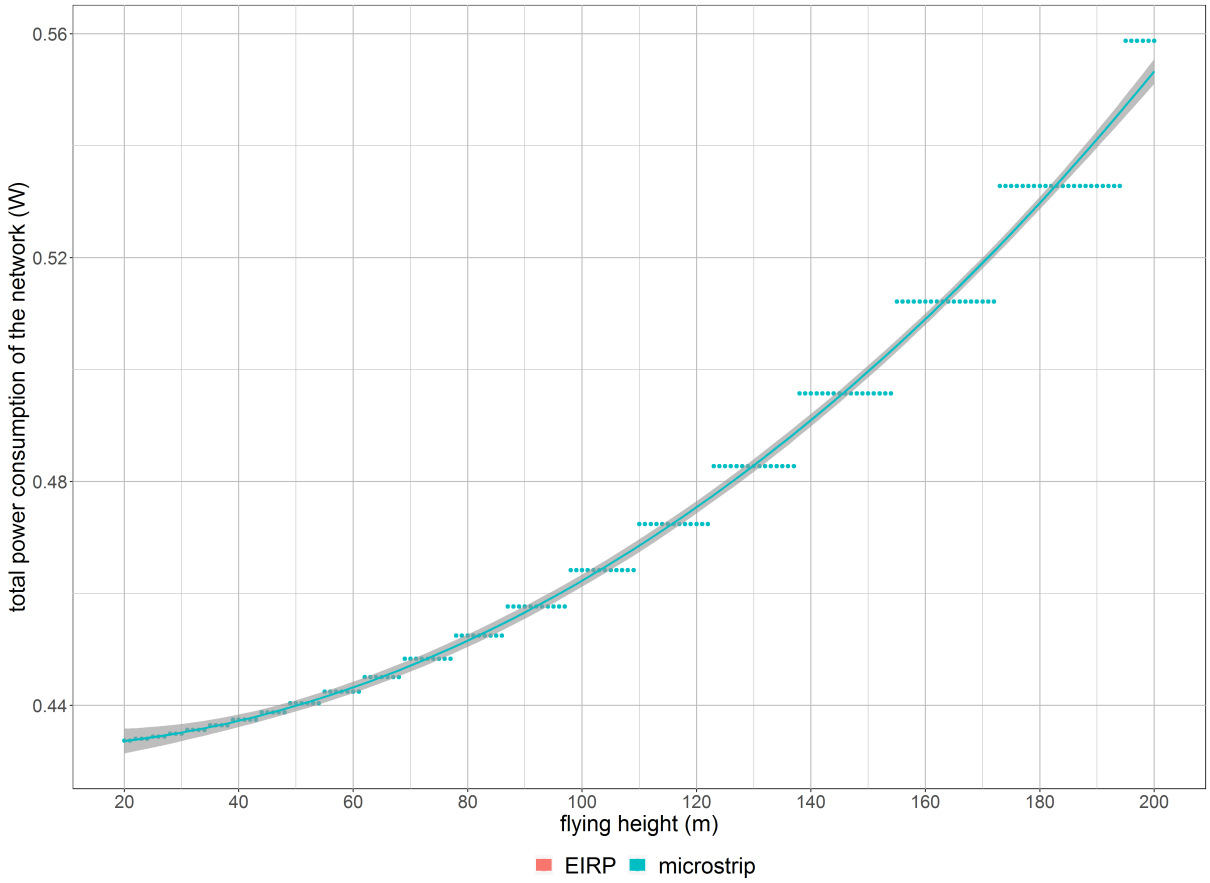

Figure 5.3: Minimal required transmission power by the antenna to reach the ground just below him. The red line shows the default maximum transmission power.

5.2 Scenario 2: Increased Traffic

This scenario has just like the previous scenario only one drone available. However, more users will be present in the network. First, a variable flying altitude is investigated for a fixed number of 224 users. Secondly, the flying height is set to 100 metres with a variable number of users. When designing the network, there will be as much possible drone locations as there are users in the network and the tool will consider all of them. It's only when the programme is finished, that one drone remains.

5.2.1 Influence of the Flying Altitude

The first case investigates how the network consisting out of one UABS behaves when applied on an ordinary day during rush hour. Different fixed flying heights are considered while 224 active users are distributed uniformly over the city center of Ghent.

A power consumption optimized network with an EIRP antenna (green) has the highest exposure. This is logical when comparing with an EIRP antenna in an exposure optimized network (red). However, when looking at figure 5.4 on the right, the power consumption in a power consumption optimized network is worse than in an exposure optimized network. To understand this, the behaviour of the deployment tool needs to be understood first. A power consumption optimized network will result in a few high powered UABSs because increasing the input power of an antenna cost less then activating a new drone. Likewise, an exposure optimized network generates a lot of low powered UABSs because the lower the antenna's power, the lower the exposure. This has the consequence that the cover radius is less and therefore requiring more drones which costs more energy. When only a limited amount of UABSs are available, like only one in this scenario, the tool will only keep UABSs which cover most of the users. Therefore is the power consumption in a power consumption optimized network way higher.

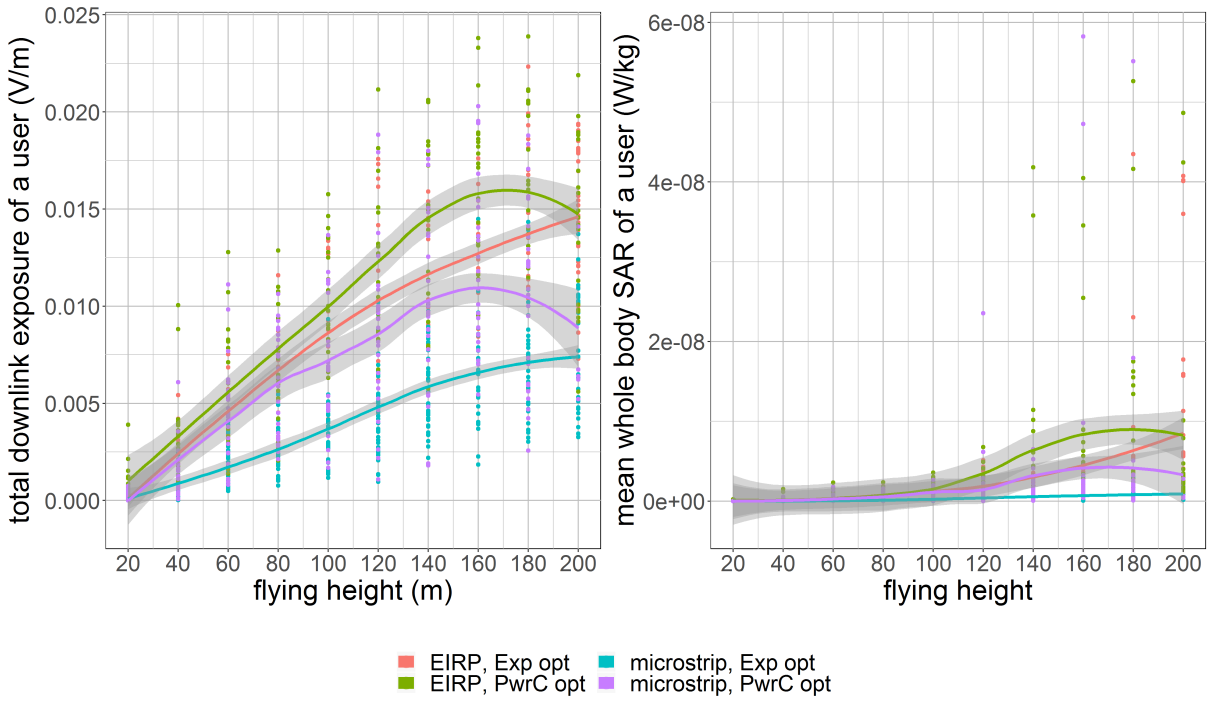

Figure 5.4: The influence of the flying height on the weighted average downlink exposure of users in the network.

The D/L exposure in figure 5.4 increases along with the flying height. One might expect a more constant behaviour like it was the case in figure 5.2 of scenario 1. To understand this, the scenario has been deducted with only two users and is illustrated in figure 5.6. The two users who will be referred to by 'red' and 'blue' are 90

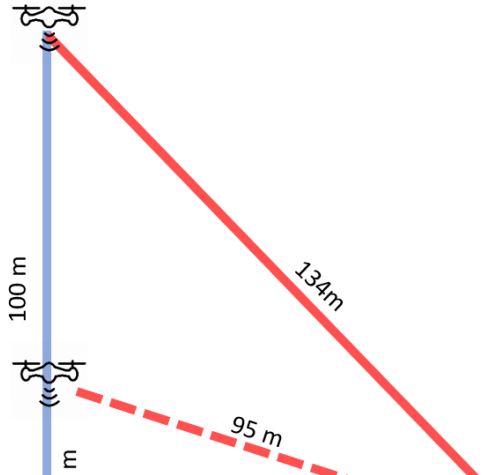

metres separated from each other with a building between them. Scenario 1 already explained that the charts can be simplified and the blue line from fig. 5.5 remains in fact constant between the zero and 130 metres. The chart shows that the UABS is positioned above the blue user. The red user is in non line of sigh (NLOS) as long as the UABS remains below 20 metres.

Once the UABS increases its flying altitude, the red user becomes into LOS but still remains uncovered. This is because the tool initially locate a possible UABS above each user and thereafter performs the fitness function. The applied fitness function must have decided that it is better to connect each user to the UABS above him. At a final state, the tool check whether the number of online drones does not exceed the capacity of the facility which is here the case. The tool therefore deactivates one UABS causing the red user to be uncovered. One could argue that the the red user should be connected to the online drone who is only 90 metres away. This would however require the online drone to increase his power consumption which would make the decisions made by the optimization strategy obsolete. When the drone flies higher, the difference in distance between both users and the base station decreases. In other words, the Pythagorean theorem shows that when the flying height

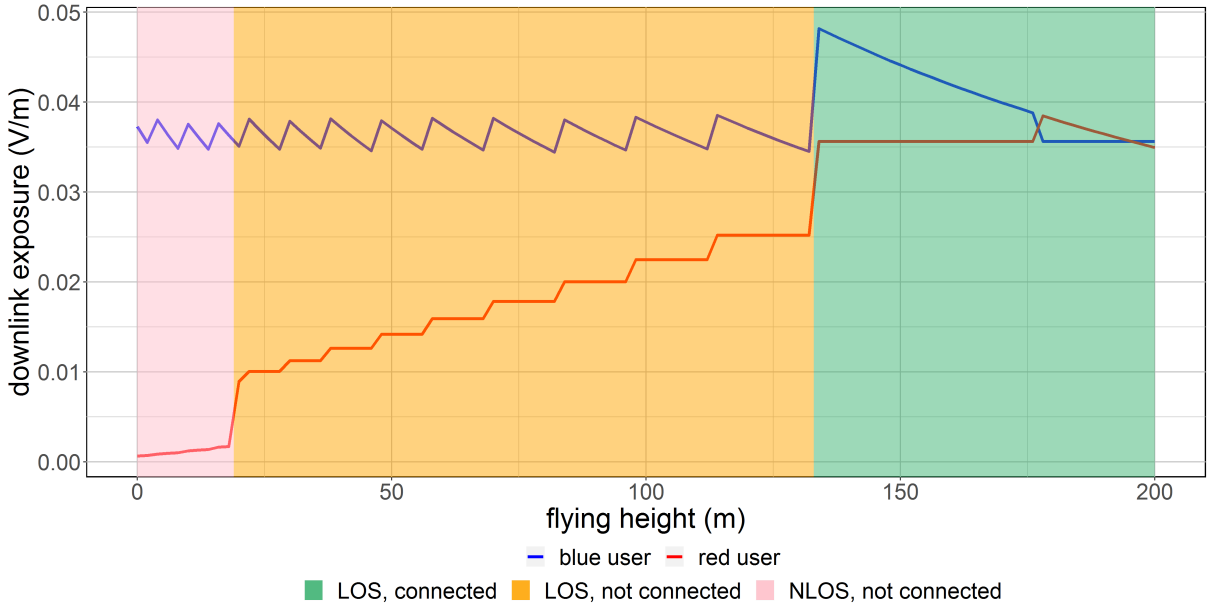

Figure 5.5: Scenario 2 with only 2 users. The coloured areas are only applicable for the red user. The blue user is connected during the entire time.

of the UABS increases, the distance with the blue user increases faster compared to the distance between that same UABS and the red user. This is also illustrated in figure 5.6. At 130 metres, the tool decides to connect both users to the same UABS. Therefore, it increases it's power consumption so the red user would have the minimal required electromagnetic exposure. This has of course a negative influence for the blue user who is way closer and experience now a much higher exposure level in fig 5.5. Around 180 metres, the red and blue line switch because the drone changes position. As explained before, the tool assigns two possible drones, one above each user. The tool must have decided that connecting both users to the other drones improves the fitness function of the entire network even though that difference might be very little. This brings us back to figure 5.4 where the electromagnetic exposure in the weighed average of all users. In other words, there are 223 users who behave like the red user while only one user behaves like the blue one. The similarity between the red line from fig. 5.5 and the electromagnetic exposure in fig 5.4 is clear.

Figure 5.7 shows that the flying height has a positive influence on the user coverage. When a UABS flies higher, there is less path loss between the user and the drone caused by buildings but also the path loss to neighbouring users decreases as explained with figure 5.5 and 5.6. Also the increasing D/L exposure from figure 5.4 from earlier indicated that the user coverage should grow. Figure 5.4 showed on the right how power consumption optimized networks in this scenario will result in higher power UABSs. And since the power consumption and therefore also the exposure of the active UABS is higher, more users will be covered compared to the exposure optimized networks.

When replacing the fictional EIRP antenna with a microstrip patch antenna, the percentage of covered users drops for both optimization strategies. This is because users who have a higher horizontal distance between themselves and the UABS, experience a higher attenuation. When a microstrip patch antenna is positioned higher, the range of the antenna increases since the angle between the user and the UABSs main lob decreases. The user will therefore experience less attenuation.

Figure **??** shows the total whole body SAR_{10g}, deducted from all electromagnetic sources. This being the exposure of all UABSs, the uplink exposure from the user's own device and the exposure of the devices from all other users. Thereafter, the weighted average of all whole body SAR_{10g} values in the network is calculated with the 50th and 95th percentile being the most important values. This is because not only the mean value is important but also users who experience higher levels of whole body SAR_{10g}.

When investigating the 3 different sources of which the total SAR-values are based on, we see that the radiation from the UABS is the main factor followed by the near field radiation from the user's own device. The far field radiation from other UE has barely influence. It looks like it is zero but it is just very low compared to the other two values and in fact does increases when

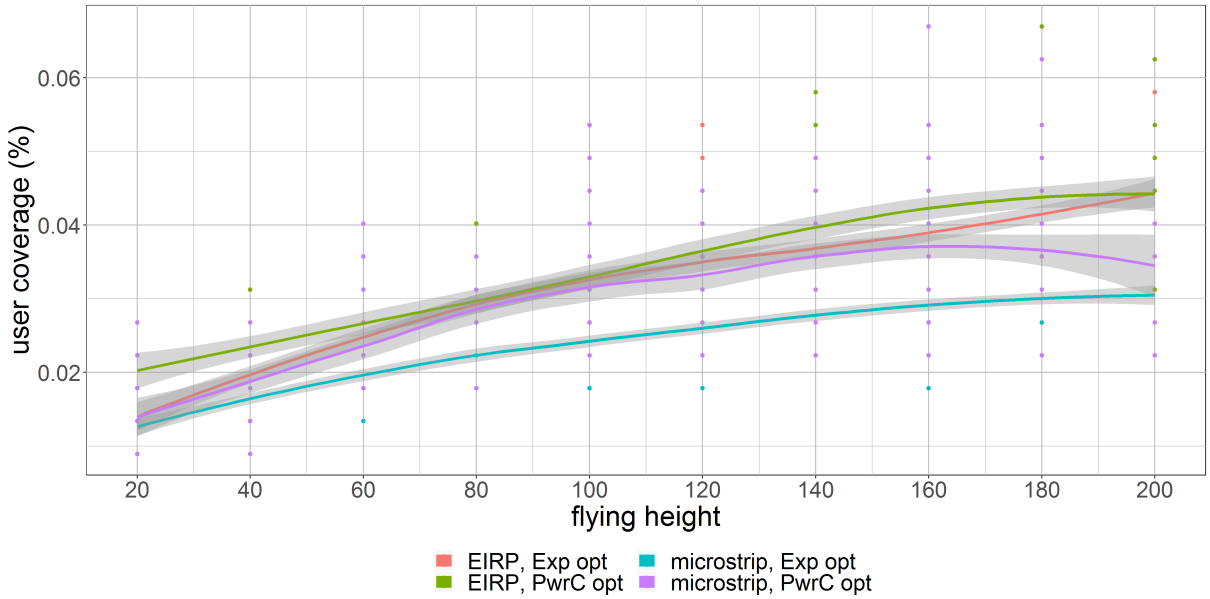

Figure 5.7: This graph shows the percentage of covered users by one drone for different flying heights.

the flying height becomes larger (just like the two other lines).

The weighted average SAR_{10g}^{ul} from the own device is zero in an exposure optimized network with a microstrip patch antenna which is even lower that the $SAR_{10g}^{neighbours}$. This is because the coverage in this scenario is so low that the weighted average only consist of uncovered users and an uncovered user his device has no power consumption.

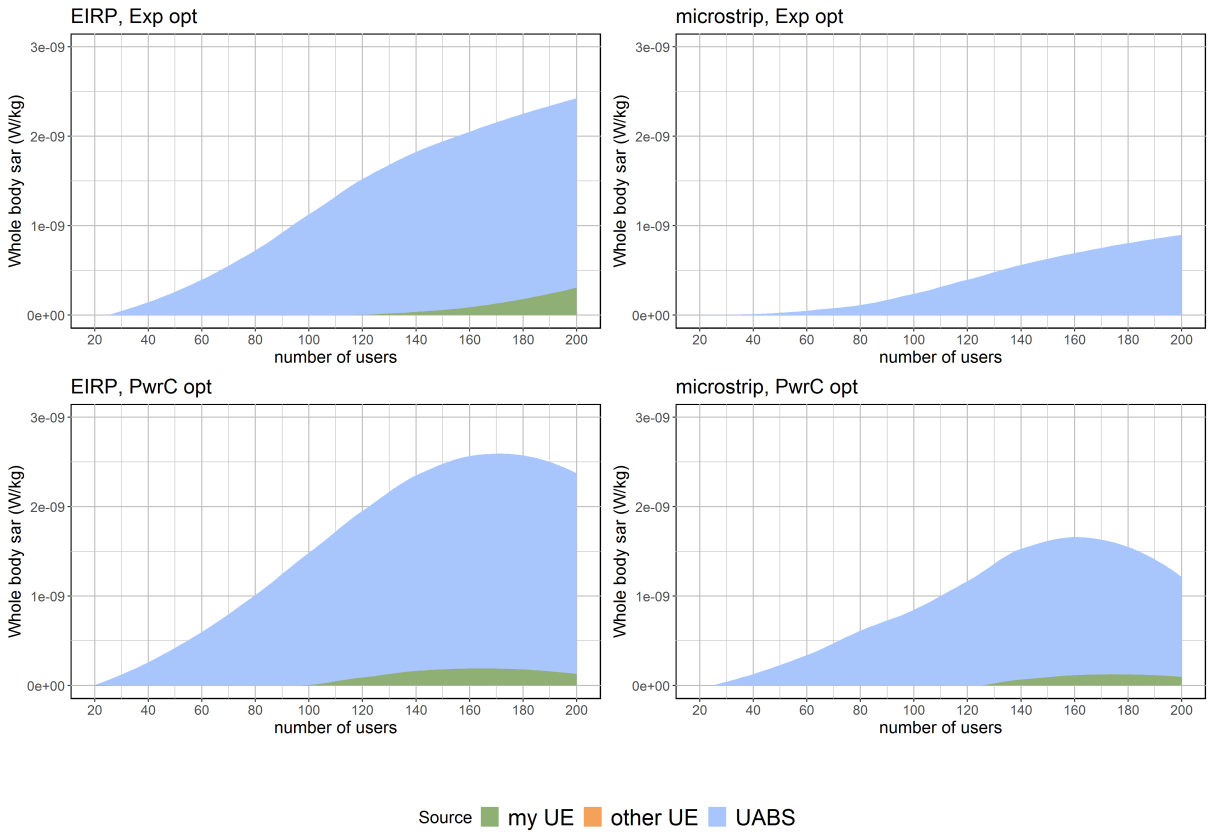

Figure 5.8: This figure shows how different sources are influenced by an increasing flying height.

5.2.2 Influence of the Number of Users

The number of covered users increase linearly compared to the number of users present in the network. This becomes clear when looking at figure 5.9 on the right. It shows how an equivalent isotropic radiator is able of reaching more users then microstrip patch antennae because of the absence of attenuation. Also, power consumption optimized networks are able of reaching more users compared to exposure optimized networks. This is because power consumption optimized network will result in few high powered base station while an exposure optimized network result in a lot of low powered base stations. This behaviour will further be explained in section 5.3

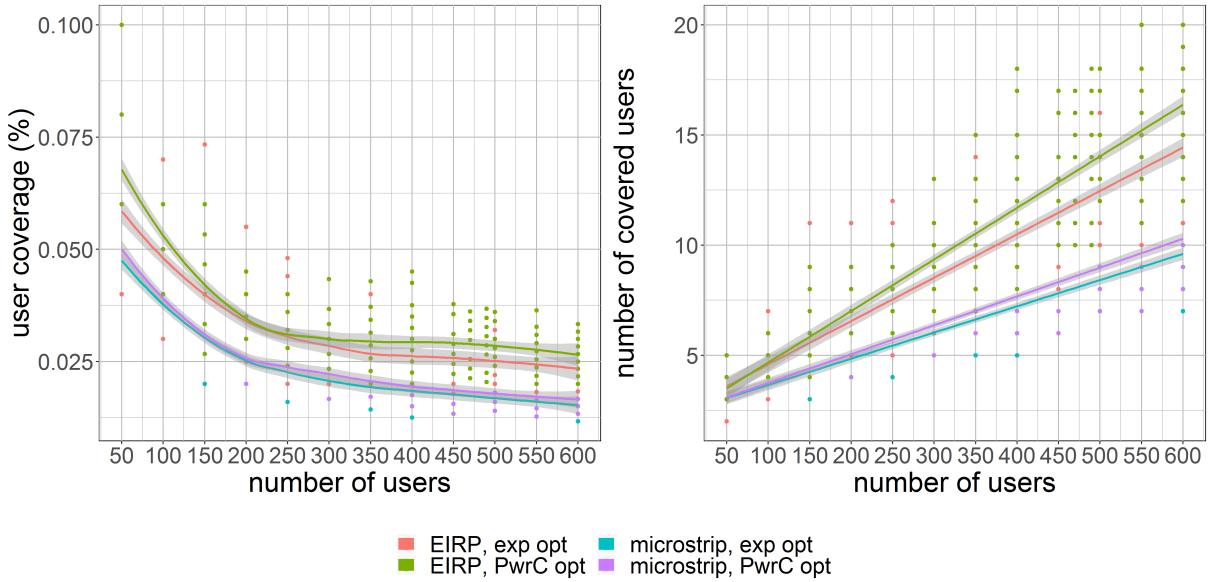

Figure 5.9: The influence of increasing traffic on user coverage.

The linear regression lines from 5.9 can be predicted with the equations in 5.2.

$$\text{number of users} = \begin{cases} y = 0,0233x + 2,3553 & \text{if EIRP and pc} \\ y = 0,0197x + 2,6144 & \text{if EIRP and exp} \\ y = 0,0131x + 2,4371 & \text{if micro and pc} \\ y = 0,0119x + 2,4652 & \text{if micro and exp} \end{cases} \tag{5.2}$$

Figure 5.9 on the left show the percentage of covered users that follows out of 5.9 on the right by taking the equations from 5.2 and dividing them by x. This results in a decreasing logarithmic behaviour because the regression lines from 5.9 have a slope of less then 0.5. So in other words, the percentage of covered users for a sparsely populated network is more compared to the percentage of users in high dense populations.

The downlink exposure is shown in figure 5.10 on the left and is directly influenced by the percentage of covered users. The average electromagnetic exposure decreases when more users become uncovered. Since an equivalent isotropic radiator in a power consumption optimized network (green) will have the highest coverage, also the D/L electromagnetic radiation from UABSs will be highest compared to other configurations. Despite the fact that the percentage of covered users decreases, the effective number of covered users increases. The power consumption of the only active UABS slightly increases in order to serve those covered users.

Figure 5.11 investigates the assets of each source contributing to the total SAR. All four config-

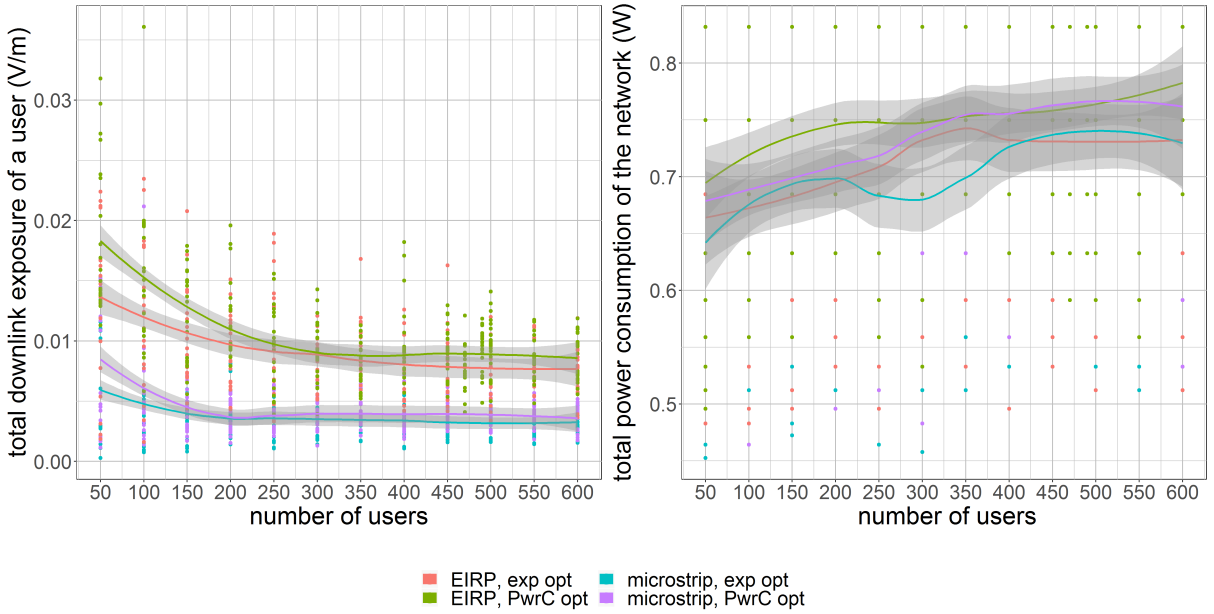

Figure 5.10: This figure shows how different sources are influenced by an increasing number of users.

urations show that for 200 users and up, base stations are the main source of electromagnetic radiation. For less users, the electromagnetic radiation from the average user's device is the dominant factor. Figure 5.9 already showed that for sparsely populated networks, a higher percentage is covered. The weighted average is thus much higher. When the population becomes more dense, more users become uncovered which decreases the weighted average of the U/L SAR. The chart also proves once again that the far field radiation from UE can be neglected. The SAR from neighbouring devices is not zero as it looks from figure 5.11 but is just really low compared to the much higher SAR-values from other sources.

While the population grows, more and more users become uncovered causing the average SAR to drop. However, this does not conclude that the same applies for users who are covered. To investigate this, a user is positioned in the middle of the city center of Ghent and a drone is positioned above him. Initially, only 49 people are active around him. The SAR of our central user is monitored while the population around him grows. Figure 5.12 shows with the black lines which users are connected. The left map is for only 50 users and shows that only one user is connected besides our central user. The map on the right is taken with 600 users and shows much more connected users.

Scenario 1 already showed that the SAR from the user's own device is only influenced by the flying height. The flying height for this experiment is fixed and the U/L SAR from his device is thus a perfect constant. The SAR from the UABS experience a slight increase. When the

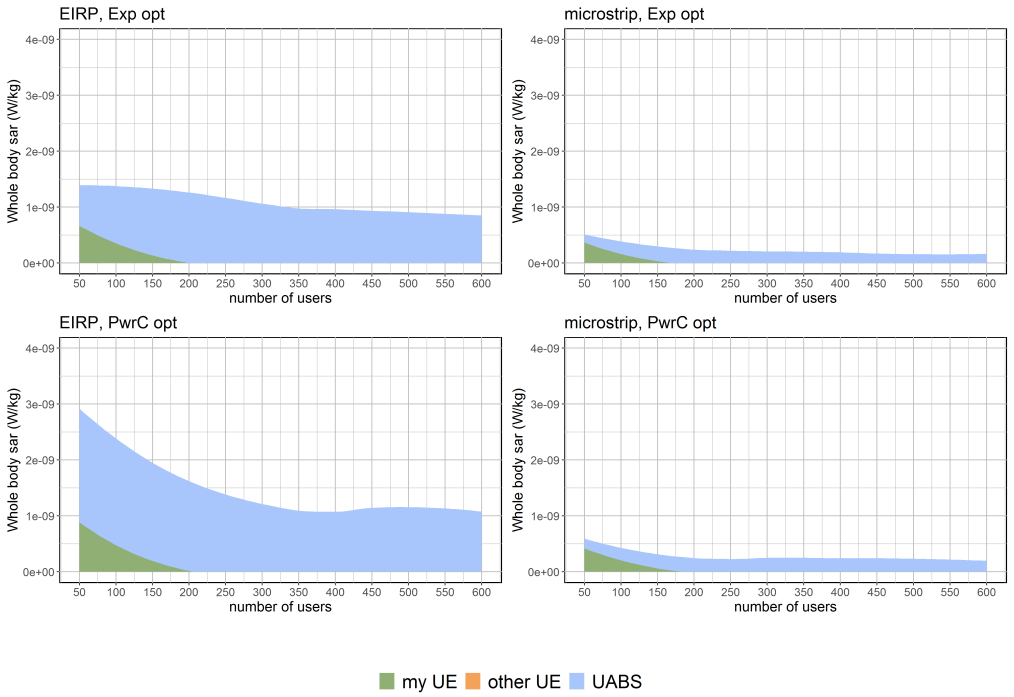

Figure 5.11: This figure shows how different sources are influenced by an increasing number of users.

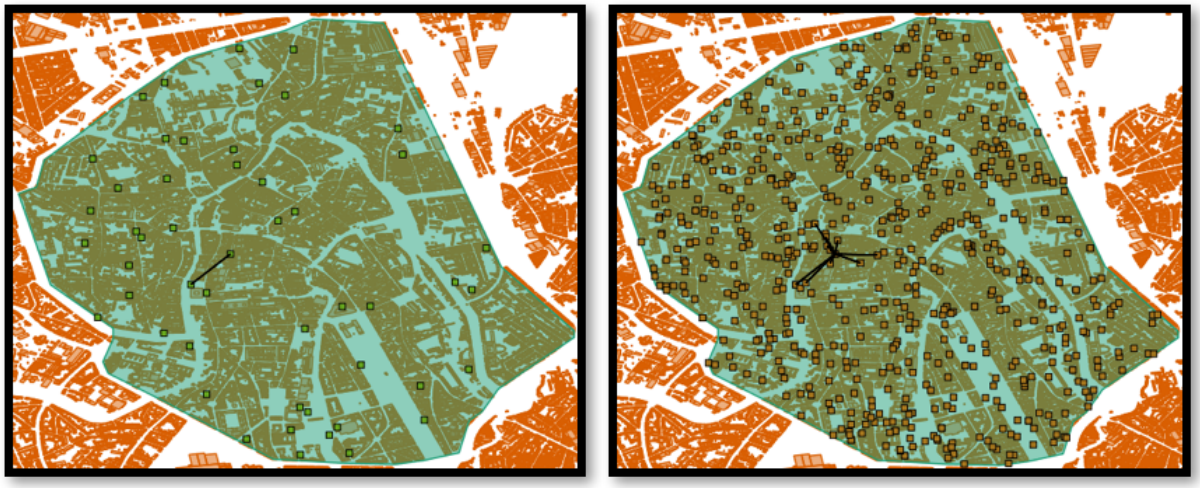

Figure 5.12: Overview of which users are connected to the UABS. The map on the left is for 50 active users while the map on the right is with 600 active users.

population increases, more users become available of which some near the central user. The UABS decides to cover also these user. These user might have a slightly worse path loss because of obstructing buildings or somewhat bigger distance. The UABS reacts to this by increasing his power consumption causing an increase in the SAR for the central user.

The far-field radiation from UE is very low as mentioned before and is therefore not visible in figure 5.12 on the left. When only looking at the right figure, we see that the SAR from other UE in fact does increase. This is normal behaviour when more and more people become available around the central user.

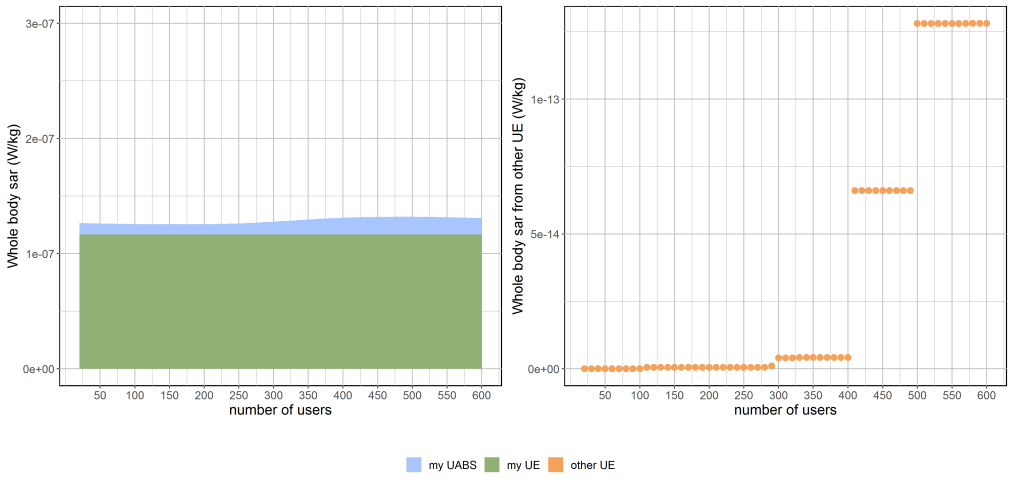

Figure 5.13: SAR-values for the user who is directly beneath the only UABS available.

5.3 Scenario 3: Unlimited Drones

This scenario has just like the previous scenario much more users in the network and investigates the same cases including the variable flying height and the variable number of users. The only difference is that the restriction of only one UABSs is dropped.

5.3.1 Influence of the Flying Altitude

The first case of this scenario examines how the network behaves for various flying heights and a fixed number of 224 users. Scenario 2 already explained that when only one drone is available, a power consumption optimized network won't result in a low powered network. In this scenario, there is no limitation on the number of drones and the network remains thus unaltered after the decision algorithm is done. Figure 5.14 clearly proves that the different optimization strategies are correctly applied by the decision algorithm and work as intended. Power consumption optimized networks have indeed a lower power consumption but therefore results in higher electromagnetic radiation. In contrast to an exposure optimized network that, as expected, will reduce the electromagnetic exposure by using more drones and thence also increasing the network's power consumption.

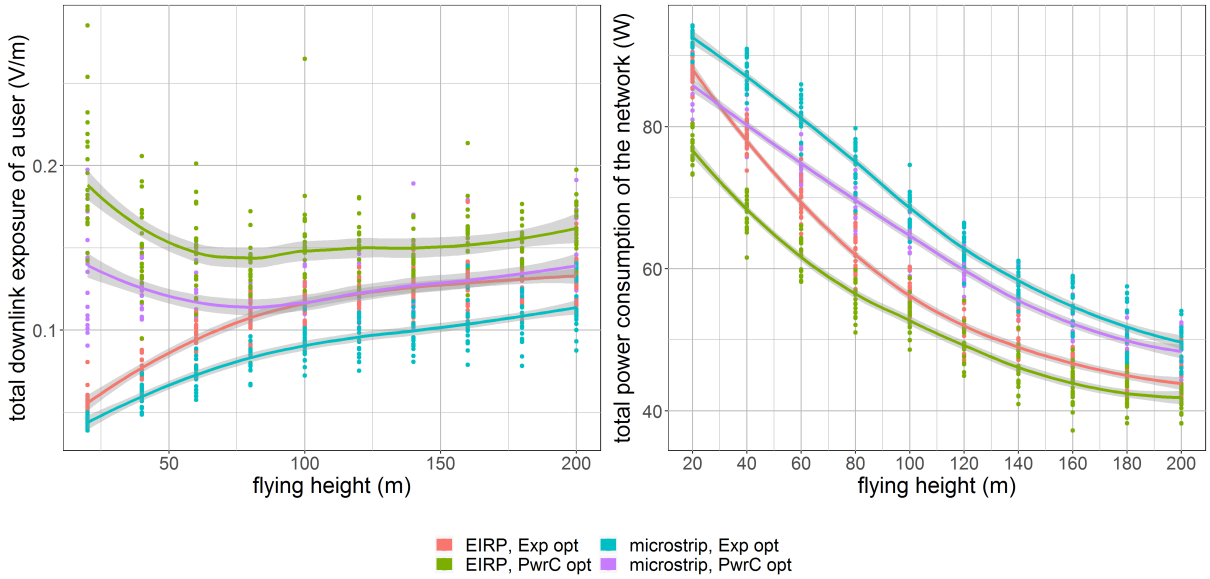

Figure 5.14: The influence of the flying height on the downlink electromagnetic radiation of the average user.. This graph shows the percentage of covered users by one drone for different flying heights.

The difference in optimization strategy is clearly bigger for low flying drones. The exposure in a power consumption optimized network starts high and decreases while an exposure optimized network behaves the opposite. This can be explained when looking at figure 5.15. At a flying height of 20 metres, the exposure optimized network has on average 220 to 224 UABSs. That is (almost) one UABS for each user so it's logical that the electromagnetic exposure is very low. The number of drones in a power consumption optimized network is much less in order to save energy but the tool still tries to reach for a 100% coverage. Since there is a high path loss from obstructing buildings, UABSs need to radiate much more to compensate for this. The exposure will thus be much higher for users in LOS. This path loss reduces when the UABSs start to fly higher then the average building and therefore decreases exposure. Also the exposure optimized network profits from the advantage of higher flying drones. Much less drones are required for only a little bit more electromagnetic exposure.

Both 5.15 and 5.14 show that the network profit from increasing the flying altitude. Not only less drones are needed but also the power consumption is lower. Both can be explained by the lower path loss when UABSs fly higher.

Scenario 1 already proved that with low flying drones, the main source of electromagnetic radiation are UABS. This changed around 80 meters where U/L electromagnetic radiation of the UE exceeds D/L radiation in order to still be able to reach the high flying UABSs. We know from previous scenarios that the behaviour of the SAR behave very similar to the downlink exposure

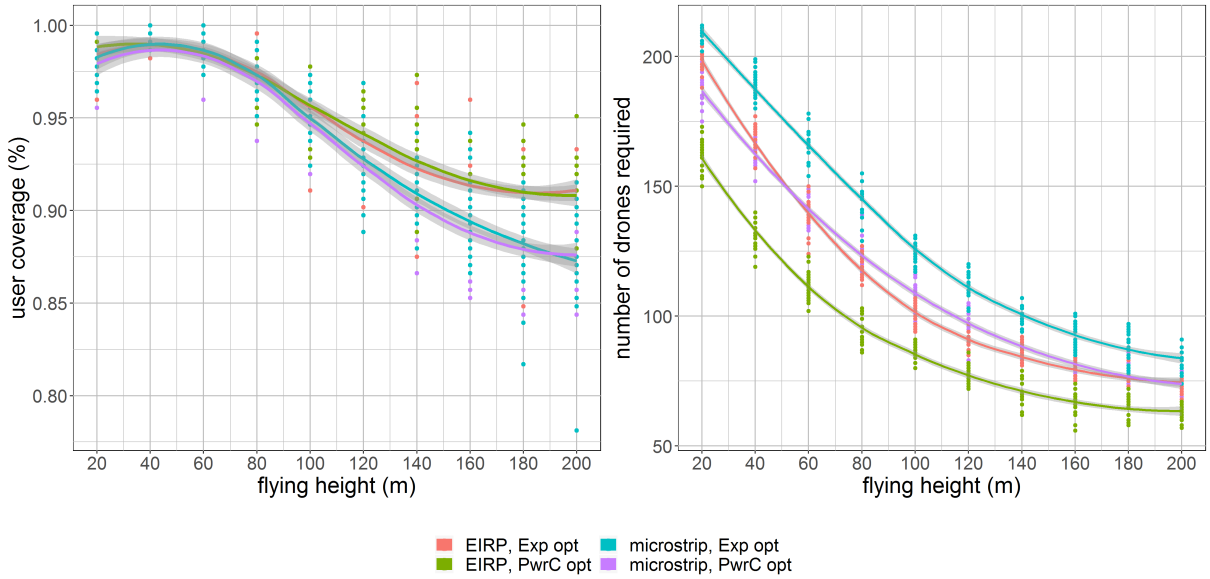

Figure 5.15: This graph shows how much drones are required for different flying heights while trying to achieve a 100% coverage.

??.

When looking at the different individual sources in 5.16, we see that SAR_{10g}^{ul} is logarithmic increasing despite the fact that figure 5.2 showed that the SAR_{10g}^{ul} increases exponentially. This was however deducted when only one user is present in the network as opposed to this scenario where 224 users are present. The covered users will still behave like in scenario 1 but fig. 5.15 shows also that less users will be covered when flying altitude increases. The average SAR_{10g}^{ul} is thus somewhere in the middle. This theory is also supported by the fact that the SAR_{10g}^{ul} in an microstrip patch antenna is less in figurer 5.16 and the percentage of covered users is also less 5.15

At a low flying altitude, users in an exposure optimized network experience significantly lower SAR-values compared to power consumption optimized networks. This difference becomes less around 70 metres. The main reason will be the path loss caused by obstructing buildings. A power consumption optimized network tries to minimize power by limiting the number of drones. Therefore, a UABS has to increase it's power level to be able to penetrate buildings. So users directly below this UABS has much higher exposure, increasing the average exposure. The UE from the user on the other side of the building has to penetrate that building as well. So the U/L SAR has to be higher as well. This behaviour is most noticeable when using an equivalent isotropic radiator because microstrip patch antennae have by default a more limited range.

Exposure from other UABSs (who are serving other users) increases when the flying height

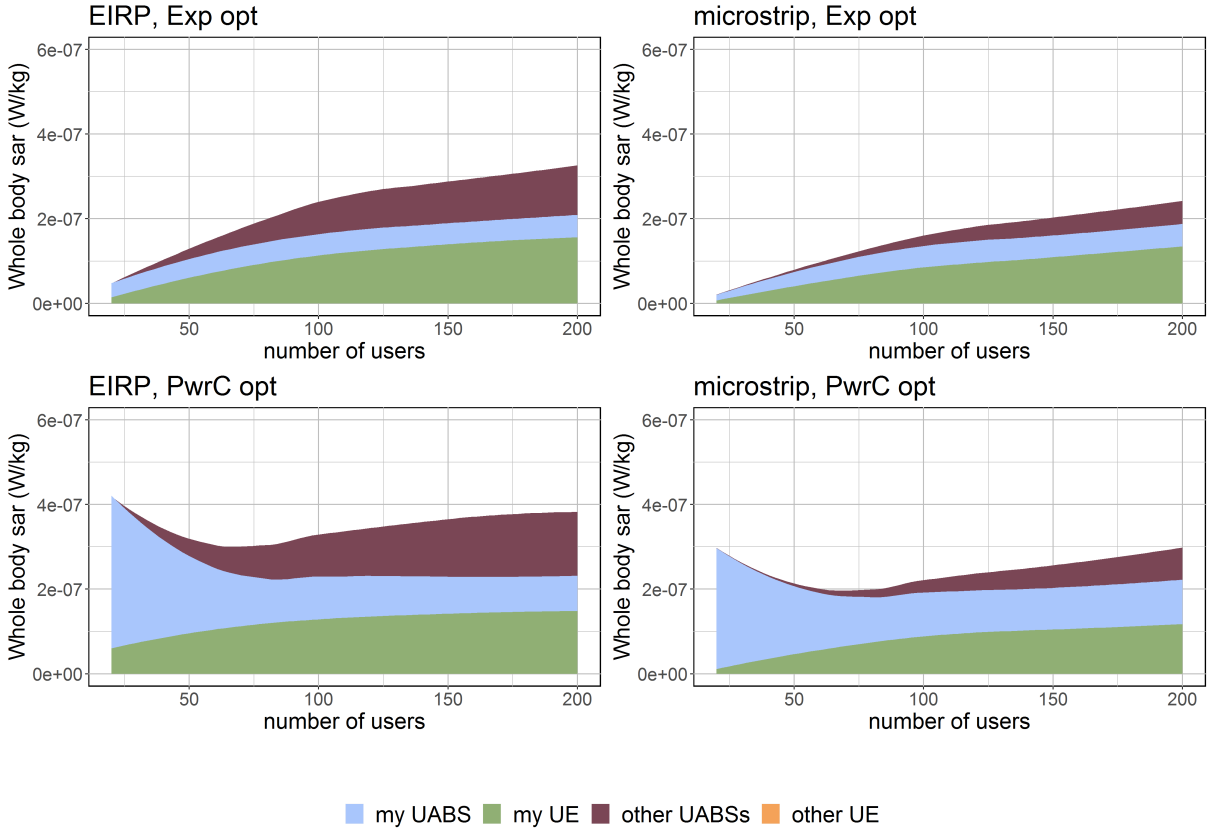

Figure 5.16: Each chart shows the total SAR to which the average user is exposed. "My UABS" stands for the UABS that is serving our average user while "other UABSs" stand for all other UABSs to which the avera user is exposed but is not served by. Other UE stand the exposure from all mobile devices that does not belong the that user.

becomes higher. Also here will the lower path loss from obstructing be the reason.

5.3.2 Influence of the number of users

The last case of scenario 3 investigates variable number of users for a fixed flying height of 100 m. There is no restriction on the number of available drones just like in the previous case meaning that there are at most as much drones as users in the network. The correct behaviour of the decision algorithm became already clear in the previous subsection 5.3.1. Also this case proves this.

Figure 5.17 shows on the left how the tool tries to reach a 100% coverage. The tool reaches this goal better for larger populations. The difference remains however very little. The tool also requires more drones for these large populations which is a logical consequence of scenario 5.2.2 where the percentage of covered users decreases for these larger populations. The difference in optimization strategy is very little for small amounts of people but increases very fast.

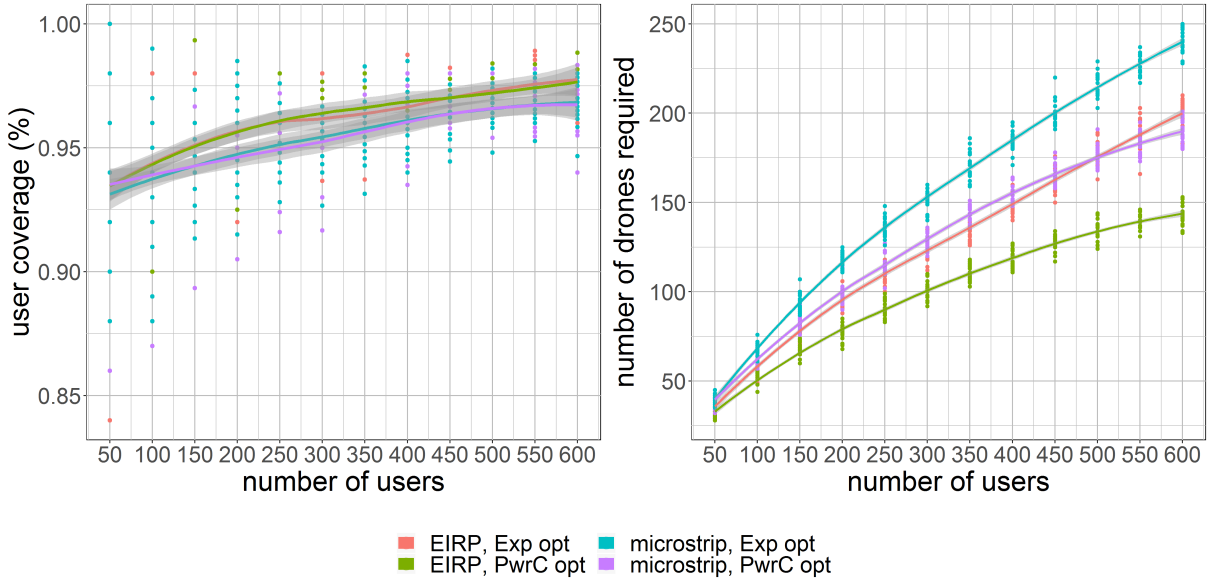

Figure 5.17: This graph shows how much drones are required for different flying heights while trying to achieve a 100% coverage.

In a scenario with 600 active users, a clear difference is noticeable between the four configurations. For instance, an EIRP power consumption optimized network requires the least amount of drones (Figure 5.17 on the right). This is logical when looking at figure 5.18 where drones in such a configuration cause the highest amount of electromagnetic radiation. This behaviour was also discussed in subsection 5.2.2.

So scenario 3 learns that a power consumption optimized network indeed result in very few drones. The average power consumption is however much higher. Scenario 2 already showed that the UABSs who were active, have a much higher power consumption. The statement that

a power consumption optimized network will result in a few high powered devices is therefore confirmed.

Likewise for an exposure optimized network. We can that the network has indeed a lower electromagnetic exposure but the power consumption of the entire network is higher. In scenario 2 became already clear that the active UABS have a low power consumption in order to guarantee low SAR values for the users. The statement that an exposure optimized network will result in a lot low powered devices is thus also confirmed.

Subsection 5.2.2 also showed how and why a microstrip patch antennae in a low powered antenna with very little coverage. This explains the behaviour of our blue line. This strategy prioritize the minimization of electromagnetic exposure. Therefore much more drones are required in order to still reach 100% coverage (Figure 5.17) and therefore requires much more energy to power all the drones (Figure 5.17 on the right). It becomes clear that more drones come with more users and therefore result in more power consumption and electromagnetic exposure.

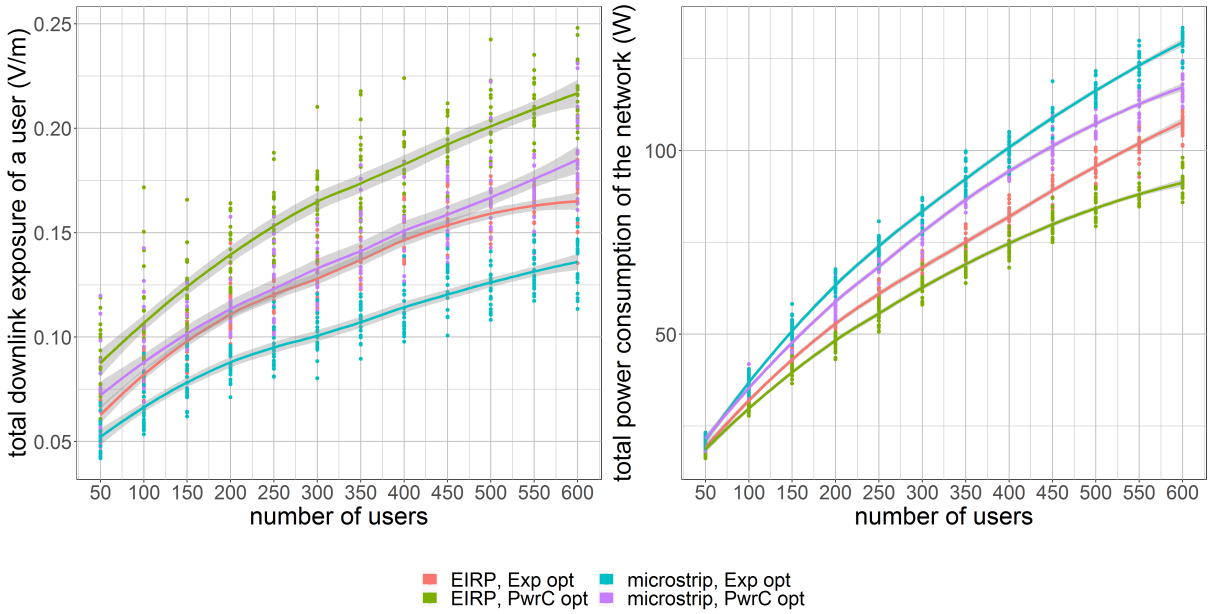

Figure 5.18: The influence of the flying height on the downlink electromagnetic radiation of the average user.

todo: pc and exp inverse linear stelling van margot bevestigen

The SAR from the serving UABS, the user's own device and other UE behave identical as it was the case with the central user from scenario 2 (section 5.2.2) in figure 5.13. The only new factor is the radiation from other UABSs who are serving other users. When more users are present in the network, more UABSs get activated. So these other UABS are the main reason the total SAR of the average user increases. The figure also shows that the decision algorithm tries to

minimize electromagnetic exposure by minimizing the exposure from other UABSs. Since the SAR-values from the user's own device and serving UABS can't decrease that much.

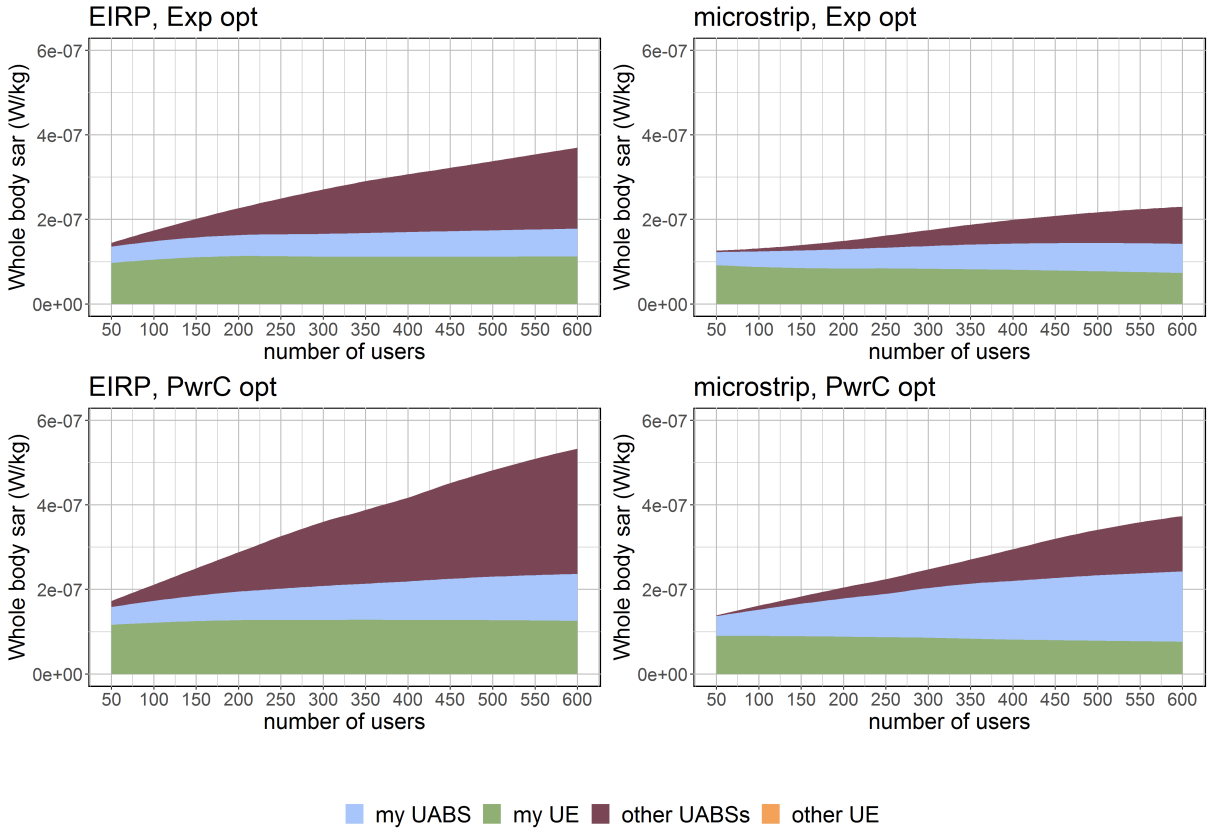

Figure 5.19: The influence of the flying height on the total power consumption of the network.

6

Conclusions

6.1 Conlusion

All conclusions are based on the default configuration as described in table 3.1 unless mentioned otherwise. Literature showed that a network can be optimized towards either the power consumption of the entire network or the electromagnetic exposure of the average user using a fitness function. This is because the power required to activate a new base station is much higher then expending it's range [10]. The fitness function was originally applied for fixed transmission towers but can also be used for UABSs as this research shows. However, the fitness function should be used with care considering that UABSs can be placed anywhere compared to the transmission towers from [10] who have a determined position. This causes that a lot of users get a UABS all by themselves in an exposure optimized network because this is the best approach to minimize exposure. A power consumption optimized network on the other hand will try to limit the number of drones in order to save energy. So as a rule of thumb: an exposure optimized network will result in a lot of low powered devices (increasing the overall power consumption) while a power consumption optimized network results in a few high powered devices (increasing the exposure of the average user). A power consumption optimized network is thus cheaper because less drones are involved. Moreover, the results show that the electromagnetic radiation in a power consumption optimized network (with high powered UABSs) is far below the thresholds enforced by the Flemish government.

The user's main sources of exposure are the user's own device and the UABS who is serving him followed by all other UABSs in the network. When the population increases, also the exposure from other people their UE increases. However, the electromagnetic exposure from these devices can be ignored compared to the much higher electromagnetic exposure from the other sources. A bigger population also cause an increase in number of drones. So when the population grows, the exposure of the user increases mainly because of a growing exposure from other UABSs that are not serving the user. Other sources barely contribute anything to the overall exposure of this user. An exposure optimized network will limits the total exposure mainly by trying to reduce the exposure from other UABSs.

An equivalent isotropic radiator has higher exposure and coverage for less power compared to realistic antennae like microstrip patch antenna. This is because of the absence of attenuation in EIRP antennae. In other words, an EIRP antenna can achieve the same coverage with less resources like power and number of drones but is unfortunately not a realistic antenna. The network will thus profit from an antenna which has a big aperture angle so the attenuation for the users on the ground would be minimal.

An power consumption optimized network has the lowest exposure around 70 to 80 metres. An electromagnetic exposure in an exposure optimized network only increases when the flying height increases. The number of required drones decrease when the flying height becomes larger. When also considering the results from [23] where an flying altitude from 80 metres is suggested for an optimal access and backhaul connectivity, a flying height of 80 metres is also here proposed for the city centre of Ghent.

In conclusion, a power consumption optimized network is proposed with a fixed flying height of 80 metres. A microstrip patch antenna with a sufficient large aperture angle is a good starting point. However, different antenna configurations should be investigated

6.2 Future work

The tool has been extended so any possible antenna in any possible direction is supported. Comparing different types of antennae is however outside the scope of this research. Conclusions on how the network performs has thus been investigated for the already existing fictional omnidirectional antenna and a realistic microstrip patch antenna. The reason for the chosen microstrip patch antenna is solely based on literature.

Bibliography

[1] "kaart van mobiel netwerkbereik." https://www.test-aankoop.be/hightech/gsms-en-smartphones/module/kaart-van-mobiel-netwerkbereik. Accessed: 03-03-2020.

[2] "Base overschreed stralingsnormen na aanslagen," *De standaard*, 2016.

[3] L. Hardell and C. Sage, "Biological effects from electromagnetic field exposure and public exposure standards," *Biomedicine and Pharmacotherapy*, vol. 62, no. 2, pp. 104 – 109, 2008.

[4] "What are electromagnetic fields." https://www.who.int/peh-emf/about/WhatisEMF/en/index1.html. Accessed: 15-10-2019.

[5] M. Deruyck, J. Wyckmans, W. Joseph, and L. Martens, "Designing uav-aided emergency networks for large-scale disaster scenarios," *EURASIP Journal on Wireless Communications and Networking*, vol. 2018, 12 2018.

[6] "Elektromagnetische velden en gezondheid: Uw wegwijzer in het elektromagnetische landschap," *Federale overheidsdienst: volksgezondheid, veiligheid van de voedselketen en leefmilieu*, vol. 5, 2014.

[7] "Normen zendantennes." https://omgeving.vlaanderen.be/normen-zendantennes. Accessed: 19-03-2020.

[8] A. Ahlbom, U. Bergqvist, J. Bernhardt, J. Cesarini, M. Grandolfo, M. Hietanen, A. Mckinlay, M. Repacholi, D. H. Sliney, J. A. Stolwijk, *et al.*, "Guidelines for limiting exposure to time-varying electric, magnetic, and electromagnetic fields (up to 300 ghz)," *Health physics*, vol. 74, no. 4, pp. 494–521, 1998.

[9] D. Plets, W. Joseph, K. Vanhecke, and L. Martens, "Exposure optimization in indoor wireless networks by heuristic network planning," *Progress In Electromagnetics Research*, vol. 139, pp. 445–478, 01 2013.

[10] M. Deruyck, E. Tanghe, D. Plets, L. Martens, and W. Joseph, "Optimizing lte wireless access networks towards power consumption and electromagnetic exposure of human beings," *Computer Networks*, vol. 94, 12 2015.

[11] D. Plets, W. Joseph, S. Aerts, K. Vanhecke, G. Vermeeren, and L. Martens, "Prediction and comparison of downlink electric-field and uplink localised sar values for realistic indoor wireless planning," *Radiation Protection Dosimetry*, vol. 162, no. 4, pp. 487–498, 2014.

[12] D. Plets, W. Joseph, K. Vanhecke, and L. Martens, "Downlink electric-field and uplink sar prediction algorithm in indoor wireless network planner," in *The 8th European Conference on Antennas and Propagation (EuCAP 2014)*, pp. 2457–2461, IEEE, 2014.

[13] S. Kuehn, S. Pfeifer, B. Kochali, and N. Kuster, "Modelling of total exposure in hypothetical 5g mobile networks for varied topologies and user scenarios," *Final Report of Project CRR-816, Available on line at: https://tinyurl. com/r6z2gqn*, 2019.

[14] D. Plets, W. Joseph, K. Vanhecke, G. Vermeeren, J. Wiart, S. Aerts, N. Varsier, and L. Martens, "Joint minimization of uplink and downlink whole-body exposure dose in indoor wireless networks," *BioMed research international*, vol. 2015, 2015.

[15] K. Kashwan, V. Rajeshkumar, T. Gunasekaran, and K. S. Kumar, "Design and characterization of pin fed microstrip patch antennae," in *2011 Eighth International Conference on Fuzzy Systems and Knowledge Discovery (FSKD)*, vol. 4, pp. 2258–2262, IEEE, 2011.

[16] I. Singh and V. Tripathi, "Micro strip patch antenna and its applications: a survey," *Int. J. Comp. Tech. Appl*, vol. 2, no. 5, pp. 1595–1599, 2011.

[17] A. Sudarsan and A. Prabhu, "Design and development of microstrip patch antenna," *International Journal of Antennas (JANT) Vol*, vol. 3, 2017.

[18] "Specific absorption rate (sar) for cellular telephones." `https://www.fcc.gov/general/specific-absorption-rate-sar-cellular-telephones`. Accessed: 27-03-2020.

[19] A. Christ, M.-C. Gosselin, M. Christopoulou, S. Kühn, and N. Kuster, "Age-dependent tissue-specific exposure of cell phone users," *Physics in Medicine & Biology*, vol. 55, no. 7, p. 1767, 2010.

[20] P. Joshi, D. Colombi, B. Thors, L.-E. Larsson, and C. Törnevik, "Output power levels of 4g user equipment and implications on realistic rf emf exposure assessments," *IEEE Access*, vol. 5, pp. 4545–4550, 2017.

[21] "Bundesamt für strahlenschutz." `http://www.bfs.de/SiteGlobals/Forms/Suche/BfS/EN/SARsuche_Formular.html`. Accessed: 14-10-2019.

[22] A. Gati, E. Conil, M.-F. Wong, and J. Wiart, "Duality between uplink local and downlink whole-body exposures in operating networks," *IEEE transactions on electromagnetic compatibility*, vol. 52, no. 4, pp. 829–836, 2010.

[23] G. Castellanos, M. Deruyck, L. Martens, and W. Joseph, "Performance evaluation of direct-link backhaul for uav-aided emergency networks," *Sensors*, vol. 19, no. 15, p. 3342, 2019.

Appendices

A

Radiation Patterns: Datasheet

Table A.1 gives an overview of the attenuation in the E and H plane. The first radiation pattern has a square groundplane with an edge of 0.060 meter while the second pattern is more of a rectangular shape with a width of 0.0524m and a length of 0.0438m. All other settings are equal as defined in 4.1.4

Table A.1: Overview of attenuation in dBm.

	pattern 1		pattern 2	
angle	E	H	E	H
0	0	0	0	0
10	-0,17	-0,14	-0.1561	-0.158
20	-0,67	-0,57	-0.5797	-0.6257
30	-1,48	-1,27	-1.263	-1.386
40	-2,57	-2,22	-2.193	-2.412
50	-3,90	-3,39	-3.357	-3.665
60	-5,40	-4,73	-4.741	-5.099
70	-7,09	-6,23	-6.337	-6.658
80	-8,82	-7,87	-8.136	-8.278
90	-10,54	-9,70	-10.11	-9.88
100	-12,20	-11,84	-12.14	-11.34
110	-13,73	-14,37	-13.81	-12.47
120	-15,04	-17,65	-14.42	-13.00
130	-16,01	-21,83	-13.72	-12.82
140	-16,47	-23,63	-12.41	-12.08
150	-16,42	-20,37	-11.15	-11.15
160	-16,05	-17,49	-10.21	-10.33
170	-15,69	-15,93	-9.683	-9.786
180	-15,54	-15,54	-9.596	-9.596
190	-15,69	-16,30	-9.963	-9.784
200	-16,05	-18,44	-10.79	-10.33
210	-16,42	-22,85	-12.07	-11.15
220	-16,47	-31,23	-13.71	-12.07
230	-16,00	-24,07	-15.25	-12.80
240	-15,03	-18,05	-15.65	-12.99
250	-13,72	-14,42	-14.3	-12.45
260	-12,20	-11,81	-12.11	-11.33
270	-10,54	-9,70	-9.882	-9.866
280	-8,82	-7,87	-7.859	-8.267
290	-7,09	-6,23	-6.069	-6.649
300	-5,40	-4,73	-4.502	-5.093
310	-3,90	-3,39	-3.154	-3.661
320	-2,57	-2,22	-2.029	-2.409
330	-1,48	-1,27	-1.138	-1.384
340	-0,67	-0,57	-0.4963	-0.6246
350	-0,17	-0,14	-1143	-0.1575

B

Radiation patterns: Example Configuration

In listing 2, a possible configuration for a radiation pattern is described. It is important to notice that this example configuration does not represent the used configuration in this master dissertation. The `radiatoinPattern`-tag consists of a `slices`-tag. This tag can contain as much slices as desired. In this example, 3 slices are defined indicated with the `attenuation`-tag. This tag contains a mandatory attribute `az` which defines the azimuth angle to which all underlying attenuation values belong. Inside the `attenuation`-tag, all attenuation values are written in a `value`-tag. Each `attenuation`-tag must contain an equal amount of `value`-tags.

The tool distributes all values equally over the 180° of that slice. In the example below, each `attenuation`-tag contains 10 values meaning that the exact attenuation is known every 20°.

The highlighted value of $-14,42$ is therefore measured at an azimuth angle of 0° and an elevation angle of 120° (counterclockwise).

```
<radiationPattern>
    <slices>
        <attenuation az="0">
            <value>0</value>
            <value>-0.5797</value>
            <value>-2.193</value>
            <value>-4.741</value>
            <value>-8.136</value>
            <value>-12.14</value>
            <value>-14.42</value>
            <value>-12.41</value>
            <value>-10.21</value>
            <value>-9.596</value>
        </attenuation>
        <attenuation az="90">
            <value>0</value>
            <value>-0.6257</value>
            <value>-2.412</value>
            <value>-5.099</value>
            <value>-8.278</value>
            <value>-11.34</value>
            <value>-13.00</value>
            <value>-12.08</value>
            <value>-10.33</value>
            <value>-9.596</value>
        </attenuation>
        <attenuation az="180">
            <value>0</value>
            <value>-0.4963</value>
            <value>-2.029</value>
            <value>-4.502</value>
            <value>-7.859</value>
            <value>-12.11</value>
            <value>-15.65</value>
            <value>-13.71</value>
            <value>-10.79</value>
            <value>-9.596</value>
        </attenuation>
    </slices>
</radiationPattern>
```

Listing 2: Example configuration of a radiation pattern.